

# We are IntechOpen, the world's leading publisher of Open Access books Built by scientists, for scientists

6,900

Open access books available

186,000

International authors and editors

200M

Downloads

Our authors are among the

154

Countries delivered to

TOP 1%

most cited scientists

12.2%

Contributors from top 500 universities



WEB OF SCIENCE™

Selection of our books indexed in the Book Citation Index  
in Web of Science™ Core Collection (BKCI)

Interested in publishing with us?  
Contact [book.department@intechopen.com](mailto:book.department@intechopen.com)

Numbers displayed above are based on latest data collected.  
For more information visit [www.intechopen.com](http://www.intechopen.com)



# Novel Chemical Vapour Deposition Routes to Nanocomposite Thin Films

Dr Russell Binions and Prof. Ivan P. Parkin  
*University College London  
United Kingdom*

## 1. Introduction

### 1.1 Nanocomposite thin films

Thin films containing nanoparticles are of interest to a wide variety of industries including but not limited to: electronics, sensing, glazing, catalysis, semiconductor and computing. The interest from these industries arises from the wide variety of properties that such composite thin films can display such as: optical, catalytic, electrical and thermal conductivity, antibacterial, Chromeogenic, photoluminescence, sorbents, plasmon resonance and colour (Green 2005; Jain et al. 2007; Walters & Parkin 2009b). Much information has been published on the synthesis of nanoparticles and ways to control their size and shape, hence properties. Much less has been written on the incorporation of such nanoparticles into composite thin films, which can then be used in useful devices.

### 1.2 Current routes to nanocomposite thin films

Current approaches to nanocomposite thin films such as sol gel routes require one or more distinct steps. These are outlined below in figure 1.

Route 1 involves the synthesis of the semiconductor matrix followed by the addition of nanoparticles in a second step. Examples of this technique include sol-gel methodologies such as spin coating or dip coating (Hida & Kozuka 2005; Yang et al. 2005).

Route 2 is similar to route 1 in that the semiconductor matrix is first constructed and the nanoparticles are formed within the film from metal ions added by a process such as high-energy ion implantation or use of a metal solution followed by heat treatment or catalytic reduction (Tzu-Hsuan & et al. 2006; Wang et al. 2006).

Route 3 is the synthesis of both nanoparticles and semiconductor matrix in a single step, for example by multi target magnetron sputtering or dual source chemical vapor deposition. Sol-gel techniques where both nanoparticle and semiconductor precursors are used has also been investigated. Liquid phase deposition has also received some attention (Houng & Huang 2006; Ko et al. 2005; Liao et al. 2006; Silva & Nicholls 2001).

Route 4 is the layer-by-layer deposition of metal particles and semiconductor material by a methodology such as multiple target laser ablation or pulsed laser deposition (Frey et al. 2006; Gyorgy et al. 2006; Serna & et al. 2006; Zorica & et al. 2006).

In routes 2-4 nanoparticles are formed in situ or concurrently with the semiconductor matrix, this significantly limits the type of nanoparticle that can be incorporated. The use of

preformed nanoparticles as in route 1 is highly desirable as a much wider range of nanoparticles can be used.

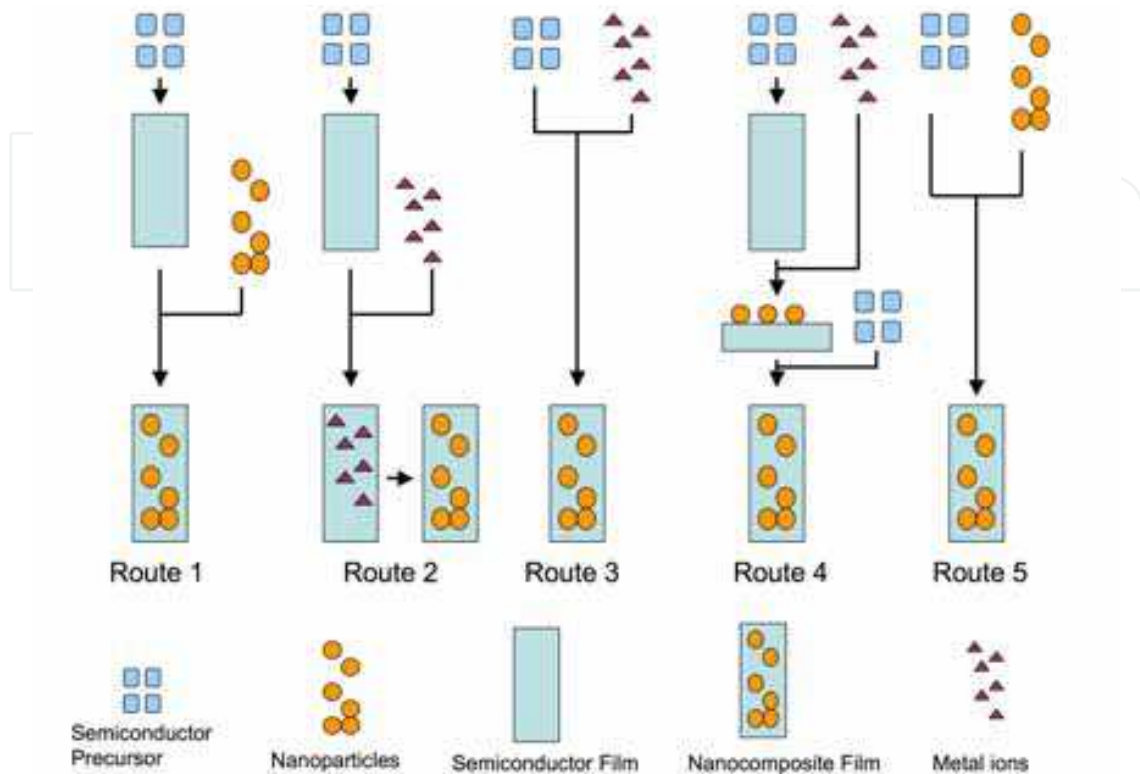


Fig. 1. Routes to nanocomposite thin films. (Palgrave and Parkin 2006)

In this chapter we will outline several different CVD approaches that allow for the deposition of nanoparticle / semiconductor composite thin films in a single step – route 5 in figure 1. The methodologies are based on the incorporation of an aerosol into the process, essentially the use of a liquid-gas aerosol to transport precursors to a heated substrate. Traditionally this approach has been taken where a conventional CVD precursor proves to be thermally unstable or involatile (Hitchman & Jensen 1993). A much wider range of precursors are available when using an aerosol delivery system. For example, exotic species such as ionic salts and metal oxide clusters have been used to deposit thin films in aerosol processes (Binions et al. 2004; Cross & Parkin 2003).

We will describe the use of colloidal suspensions as precursors towards nanocomposite thin films. In many ways colloidal suspensions are the antithesis of a CVD precursor, which normally requires volatile molecular species. The use of an aerosol allows for the transport of preformed nanoparticles, these may be incorporated into a conventional CVD flow (hybrid CVD) or transported with another semiconductor precursor (aerosol assisted CVD or AACVD)

There are three main benefits to these techniques over others. First, they are flexible: many preformed nanoparticle solutions can be used, and combined with any chemically compatible precursor, to produce a large range of nanocomposite films. Second, CVD is a widely used industrial technique in fields such as microelectronics and glazing, and it has a number of well-known advantages, not least the deposition of adherent, conformal films. Thirdly these techniques are relatively simple one step processes that do not require ageing times or special handling steps.

### 1.3 Chemical vapour deposition

All CVD processes have a number of common steps (illustrated in figure 2) these are:

1. Precursor, generation of active gaseous reactant species.
2. Transport, delivering the precursor into the reaction chamber.
3. Adsorption of the precursor onto the hot surface.
4. Decomposition of the precursor to give the atom needed for the film and organic waste.
5. Migration of atoms to a strong binding site.
6. Nucleation that leads to the growth of the thin film.
7. Desorption of unwanted side products.
8. Removal of unwanted products.

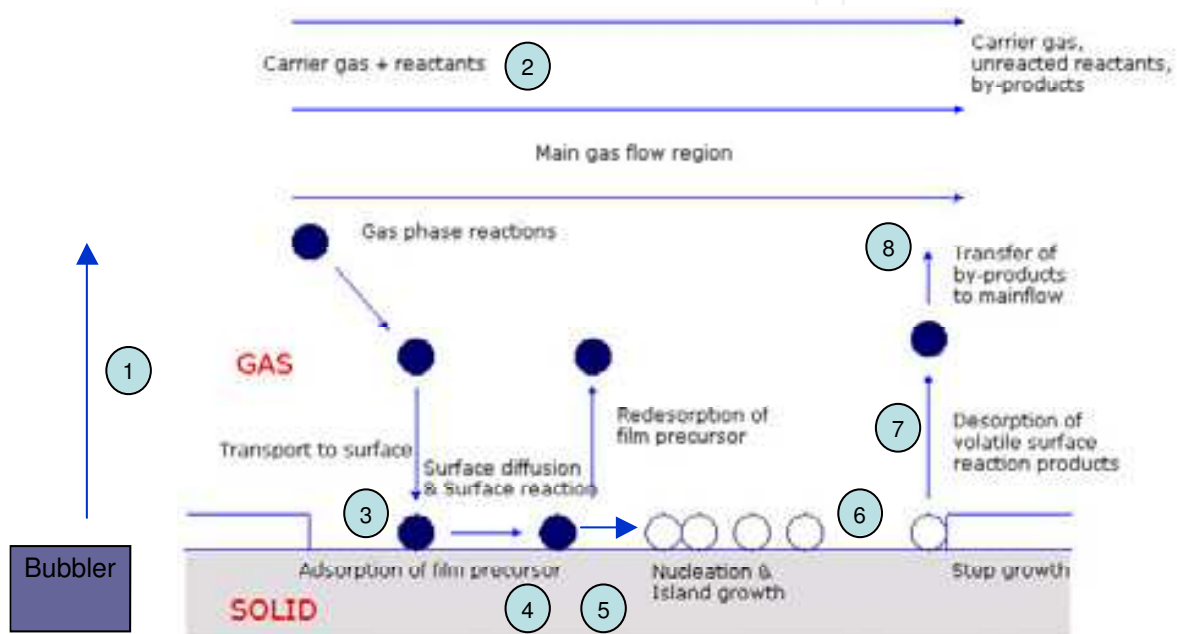


Fig. 2. Diagram to show the pathway of CVD reactions adapted from (Hitchman & Jensen 1993).

#### 1.3.1 Precursor, generation of active gaseous reactant species.

The selection of a suitable precursor is essential for the process. For traditional CVD processes the precursor must be highly volatile in order to ensure enough partial pressure so that it can easily be promoted into the gas phase. If the precursor is a liquid or a powder this can be achieved using a heated bubbler. The precursor must also be stable in the bubbler and during gas phase transport only reacting with the heated substrate. As with all chemical synthesis it is desirable for the precursor to be readily available at high purity and at a reasonable price.

#### 1.3.2 Transport, delivering the precursor into the reaction chamber.

Delivery is via an inert carrier gas (e.g.  $N_2$  (Kuroda et al. 1989) or Ar), a reactive gas (e.g.  $O_2$  (Miao et al. 2005) or  $H_2$ ) or a mixture of the two. Inert carrier gases are the most commonly used as they transport the precursor into the reaction chamber without significantly affecting the properties of the deposited film. Oxygen can be used as a reactive carrier gas to oxidise the precursor to form a metal oxide thin film. Using a mixture of oxygen and

nitrogen, the stoichiometry of the metal oxide formed can be controlled by changing the concentration of the gases. There have also been complex examples using mixtures of reactive carrier gases such as (e.g. Ar-N<sub>2</sub>-BF<sub>3</sub>-H<sub>2</sub>) (Zhang et al. 2002)

### 1.3.3 Adsorption of the precursor onto the hot substrate.

The hot surface required for CVD is essential to overcome the energy barrier of reaction. Both hot and cold wall reactors can be used. A cold wall CVD reactor is where the substrate is the only piece of apparatus heated and deposition occurs only on the substrate. However, in hot wall CVD the entire reactor is heated. This clearly means the deposition can occur on the walls as well as the substrate, which can result in wastage of precursor. However, it also ensures that the heat distribution across the substrate is completely even helping to deposit a more consistent film. The use of a hot wall reactor also mitigates the affects of thermophoresis. Thermophoresis is a phenomenon where particles (such as aerosol droplets) experience a force in the direction of a temperature gradient, this is where they are directed away from the heated substrate leading to a less adhesive film (Hampden-Smith & Kodas 1999).

### 1.3.4 Decomposition and reaction of the precursor.

The decomposition of the precursor can occur in the gas phase or on the substrate surface. If reaction happens in the gaseous phase the precursor may "snow" onto the surface creating a weaker and lower density film. If this occurs there are also other problems that can occur such as pin hole defects in the film surface. In some cases the gas phase reaction can be fundamental to the film growth mechanism, e.g. a gas phase adduct in the formation of Tantalum phosphide (Blackman et al. 2003) If however the dissociation of the intermediate does not occur until in contact with the surface, the material required for a film; often a metal, or metal oxide, separates itself from the organic part, e.g. the formation of a WO<sub>3</sub> thin film from WCl<sub>6</sub> with O containing reactive solvents (Blackman & Parkin 2005).

### 1.3.5 Migration of atoms to a strong binding site.

This is where a chemical reaction with the surface takes place changing the process from physisorption to chemisorption. The surface species target an activated site e.g. a defect site or step site where the energy needed to bind is lower.

### 1.3.6 Nucleation leading to film growth.

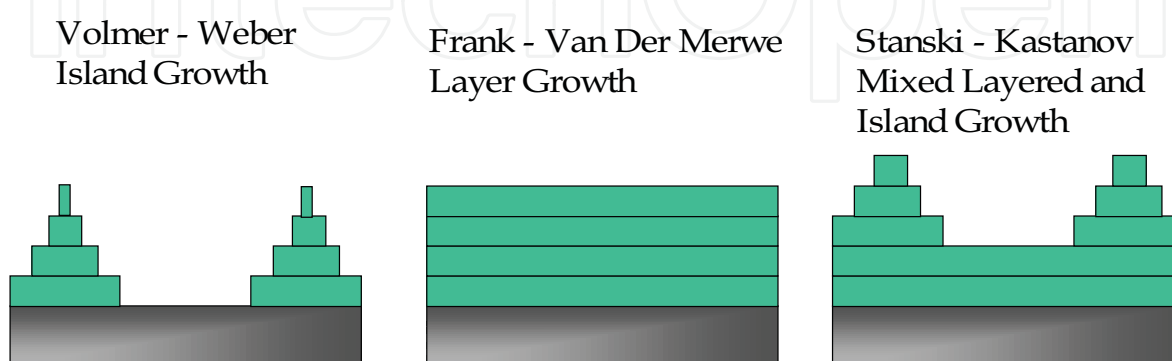


Fig. 3. Diagram to show different growth mechanisms within CVD adapted from (Binions 2009).

There are three main types of film growth mechanisms in CVD (Figure 3.). The determining factor by which the growth occurs is due to the affinity of the precursor to the substrate and the precursor flux to the substrate. If the bond formed between the precursor and the substrate is stronger then layer-by-layer growth is more likely. If however the precursor-to-precursor bond is stronger island growth occurs. Stranski-Krastanov (Michael L. Hitchman 1993) growth occurs when both growth types occur either layer growth followed by island growth, or island growth followed by layer growth.

## **1.4 Chemical vapour deposition for nanocomposites**

### **1.4.1 Plasma enhanced chemical vapour deposition**

Plasma enhanced chemical vapour deposition (PECVD) can be characterised as when a plasma, created by an intense electric field, is used to activate precursor species before they reach the surface of the substrate. This high intensity field interacts with gaseous electrons and accelerates them; this causes the electrons to collide with precursor species and potentially ionise them. The field also interacts with ions but because of the larger mass of these, has a significantly lesser effect.

PECVD has been used in two distinct ways to synthesise nanocomposite materials. The first of which is to coat commercially purchased titanium dioxide nanoparticles that were then attached to a silicon wafer substrate. Polymeric coatings were produced from a variety of different plasmas, the most useful of which was HMDSO (hexylmethyldisiloxane) and  $O_2$ . The coatings were conformal and enabled coated nanoparticles to stay dispersed in solution for longer periods of time (Shearer et al. 2010).

PECVD has also been used to prepare diamond like carbon (DLC) thin films that have also been grown containing nanoparticles, notably gold or titanium oxides. DLC and the nanoparticles are found using electron microscopy to deposit as segregated phases. This allows the size of the nanoparticulate agglomerate to control properties such as surface roughness and hydrophilicity in the case of titanium dioxide and film colour in the case of gold. The use of gold nanoparticles in these composites leads to the observation of a surface plasmon resonance (SPR) in the UV/visible spectrum. It was found that the SPR centre could be controlled by careful consideration of the gold concentration in the gas phase. A higher proportion of gold led to larger gold nanoparticle agglomerates and a subsequent red shift in the colour of the film from 550 nm to 570 nm (Paul et al. 2009).

### **1.4.2 Direct liquid injection**

Direct liquid injection (DLI) is a relatively new development in precursor deployment where a liquid phase precursor is introduced into the CVD reactor system in a systematic and controlled manner, often involving flash evaporation of the liquid precursor in the gas stream, a schematic of the setup is depicted in figure 4. DLI CVD has had limited use in the production of nanocomposite thin films; only having been used to introduce metal nanoparticles into thin films of  $TiO_2$  with a view to producing antibacterial films.

Maury et al. grew nanocomposite thin films of  $TiO_2$  containing copper nanoparticles using titanium tetraisopropoxide (TTIP) and copper bis (2,2,6,6-tetramethyl-3,5-heptadionate),  $Cu$  (THMD)<sub>2</sub>, as organometallic precursors. Liquid solutions of the precursors were prepared in xylene and were injected into the CVD reactor system via a flash evaporation chamber. Nanocomposite thin films were deposited at 683 K on glass, silicon and steel substrates. Electron microscopy revealed that the copper was incorporated as metal particles with diameters between 20 and 400 nm. The authors note that the incorporation of larger

fractions of copper nanoparticles led to a higher anatase content in the TiO<sub>2</sub> matrix and a higher antibacterial activity (Mungkalasiri et al. 2009).

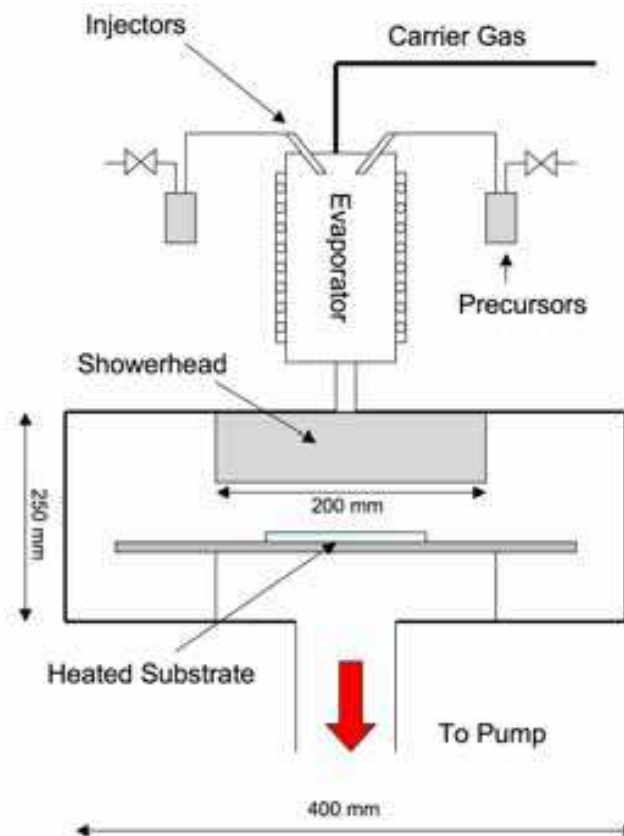


Fig. 4. Schematic of the direct liquid injection chemical vapour deposition system adapted from (Mungkalasiri et al. 2009).

The same group examined the production of nanocomposite thin films of TiO<sub>2</sub> containing silver nanoparticles grown from TTIP and silver pivalate using the same experimental setup. Silver nanoparticles were observed during transition electron microscopy with a diameter range of 5 - 10 nm, somewhat smaller than comparable nanocomposite produced by sol-gel methodologies [ref]. The films were found to be bactericidal with an Ag/Ti ratio of 0.15 and above. The films were also investigated for their photocatalytic activity and compared with a plain TiO<sub>2</sub> film grown under the same conditions. The incorporation of silver nanoparticles into the matrix reduced the photocatalytic activity of the nanocomposite thin films compared to the plain film and higher doping levels (Ag/Ti > 0.1) leads to photocatalytic inactivation (Mungkalasiri et al. 2010; Page et al. 2007).

### 1.4.3 Atmospheric pressure chemical vapour deposition

Atmospheric pressure chemical vapour deposition (APCVD) has been used to investigate the production of thermochromic nanocomposite thin films by Parkin et al. in a series of papers investigating the dual deposition of VO<sub>2</sub> and TiO<sub>2</sub> or SnO<sub>2</sub> (Manning et al. 2005; Qureshi et al. 2006; Qureshi et al. 2004).

Vanadium dioxide films were synthesised from the atmospheric pressure chemical vapour deposition reaction of vanadium oxychloride (VOCl<sub>3</sub>) or vanadium tetrachloride (VCl<sub>4</sub>) and water. The formation of a nanocomposite thin film was achieved by codeposition with

another metal oxide precursor that reacted at a faster rate than the vanadium precursor,  $\text{SnCl}_4$  and  $\text{Ti}(\text{O}^i\text{Pr})_4$  were utilised for this purpose (Manning et al. 2005).

The titanium dioxide and vanadium dioxide nanocomposites were formed from the codeposition of  $\text{VCl}_4$  and  $\text{Ti}(\text{O}^i\text{Pr})_4$  at 650 °C. The nanocomposite thin films contained two major crystal morphologies on inspection by scanning electron microscopy, the first, rectangular like deposits of vanadium dioxide 3  $\mu\text{m}$  x 200 nm in size, the second approximately spherical deposits of titanium dioxide of varying diameters. The films were found to have both thermochromic properties, with a metal semiconductor transition occurring at 54 °C and photocatalytic properties, albeit with activity at a 10% level of a plain anatase titanium dioxide film used for comparative purposes (Qureshi et al. 2006).

Tin dioxide and vanadium dioxide thin films were prepared from the codeposition of  $\text{SnCl}_4$  and  $\text{VCl}_4$  at 625 °C. The films had a morphology of 50 nm particles aggregated into larger islands some 200 nm in diameter. Energy dispersive analysis of X-rays (EDAX) indicated that tin was present throughout the films, but that vanadium was present in only trace, a few atomic percent, levels (Qureshi et al. 2004).

The authors advance the theory in this paper that nanocomposites are formed rather than solid solutions when both metal precursors have fast gas phase reaction rates. In this instance the oxygen precursor (water in this case) is used up much more quickly to generate segregated metal oxide islands on the substrate surface and a nanocomposite is observed with segregated oxide phases. In the alternative example, where there is a significant difference between metal precursor gas phase reaction rates e.g.  $\text{VCl}_4$  and  $\text{WCl}_6$  a solid solution of the less reactive precursor metal is formed in a metal oxide film of the more reactive precursor,  $\text{V}_{1-x}\text{W}_x\text{O}_2$ , as molecules of the less reactive metal precursor become trapped in the growing metal oxide film and become incorporated into the crystal structure.

## 2. Aerosol assisted chemical vapour deposition of nanocomposite thin films

### 2.1 Introduction to AACVD

Aerosol assisted chemical vapour deposition (AACVD) is based on a liquid – gas aerosol to transport soluble precursors to a heated substrate. The method has traditionally used where conventional CVD techniques have proved inadequate; for example when an APCVD precursor is involatile or thermally unstable (Hitchman & Jensen 1993). The requirements of precursors for AACVD are somewhat different than those for other CVD techniques; the restrictions of volatility and thermal stability are removed. Indeed the most important consideration for AACVD precursors is solubility, which allows a wide variety of unusual precursor systems and materials to be investigated including metal oxide clusters and ionic thin films (Binions et al. 2004; Cross & Parkin 2003).

The AACVD system has several advantages compared to other systems. Firstly it is enormously flexible. A wide variety of precursor solutions can be used; changing the content of the precursor flask can control film doping and a wide variety of solvents can be utilised (Parkin et al. 2008). Further to this precursor solutions may contain preformed nanoparticles or nanoparticle suspensions that can be deposited along with any chemically compatible precursor to produce a wide range of nanocomposite thin films. Secondly, CVD is a widely used industrial technique in fields such as microelectronics and window coating and has a number of well-known characteristics such as the production of adherent and conformal films (Jones & Hitchman 2009). AACVD has the potential to be inexpensively incorporated into current processes for the production of thin film nanocomposites.

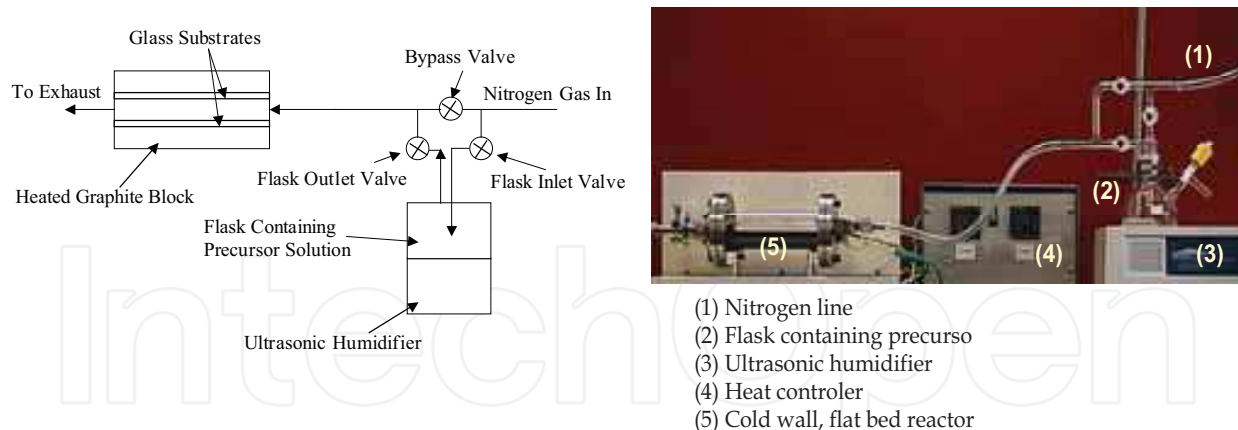


Fig. 5. Schematic (Left) and photograph (Right) of the AACVD system.

The typical AACVD set up involves five key parts (as shown in figure 5). The system must contain a carrier gas; typically this is an inert gas such as nitrogen or argon although a reactive gas such as oxygen could be used. Second, the system must contain a precursor source such as a flask with precursor inside. Third, a method of generating an aerosol of the precursor solution and carrier gas, this can be done by forced wave ejection using a humidifier, atomisation using a spray nozzle or similar. Fourth, a method of controlling the temperature of the system and finally a reaction chamber, which may be hot or cold wall depending on the precursor system to be used, the size of the aerosol particles and the desirability or otherwise of thermophoretic effects.

Several key variables can be controlled in AACVD, these are; carrier gas flow rate. Controlling the flux of solvent and precursor to the substrate can have pronounced affects on not just the flow conditions (laminar versus turbulent) but also on the surface chemistry and precursor decomposition pathways and subsequent incorporation of impurities into the film. Precursor flask composition is important in controlling the final film composition; in AACVD a simple change in the ratio of precursors in the flask has proven to be a reliable way to control deposited film composition. The substrate temperature may be controlled and as in any CVD reaction is important for determining the surface chemistry and film growth energetics. It is also important along with aerosol particle size, which can be controlled by changing nozzle or humidifier operating frequency, in suppressing or encouraging thermophoresis. (Piccirillo et al 2008)

## 2.2 AACVD of nanocomposite thin films

AACVD has been used for the production of nanocomposite thin films since 2006 (Palgrave & Parkin 2006). Palgrave et al. described the production of nanocomposite thin films of titanium or tungsten oxides encompassing gold nanoparticles. This was the first example of a thin film nanocomposite being grown using AACVD from a preformed nanoparticle solution. The ratio of gold precursor to metal precursor in the precursor flask was demonstrated to control the final film composition. The addition of gold nanoparticles into the films led to the observation of a surface plasmon resonance band in the UV/Vis spectra. In the same year Gleason et al. combined ultrasonic atomization and plasma enhanced CVD to produce nanocomposites of silicon dioxide and dextran.

The deposition of  $\text{Cr}_2\text{O}_3$  based nanocomposites incorporating fullerene like tungsten disulfide nanoparticles for the production of wear resistant thin films was studied by Choy

et al. The authors demonstrate the facile production of nanocomposite thin films using this method and report that the coefficient of friction of the films is reduced by some 30% on the incorporation of the nanoparticles. The film contact angle was significantly changed from hydrophilic ( $8^\circ$ ) for plain  $\text{Cr}_2\text{O}_3$  to hydrophobic ( $105^\circ$ ) for the nanocomposite thin film (Choy & Hou 2008; Ross and Gleason 2008).

AACVD has been demonstrated by Quershi et al. to transport and deposit nanoparticulate powders as long as they could be adequately dispersed in solution. The use of "aerosol assisted deposition" allowed for a thin film of  $\text{WO}_3$  to be synthesised from a dispersion of  $\text{WO}_3$  nanoparticles in toluene. The films were deposited alongside TTIP in order to make a titanium dioxide and tungsten trioxide nanocomposite thin film. The films were found to have an unusual crenulated morphology that was not possible to recreate using other techniques such as sol-gel or APCVD. The presence of  $\text{WO}_3$  could not be detected using X-ray diffraction or Raman and the films retained both photocatalytic ability and hydrophobicity (Quershi et al. 2007).

Quershi et al. have also examined the deposition of titanium dioxide and titanium dioxide nanocomposites using AACVD (Quershi et al. 2009). TTIP was used as a titanium precursor and dissolved in toluene, whilst a commercially sourced cerium dioxide nanopowder aqueous suspension was used to deposit cerium dioxide. The two precursors were deposited alternately to form layers of titanium dioxide and cerium dioxide on glass substrates. The resulting films consisted of islands of titanium dioxide approximately 150 nm in diameter covered in cerium dioxide nanoparticles between 10 and 15 nm in diameter (Figure 6).

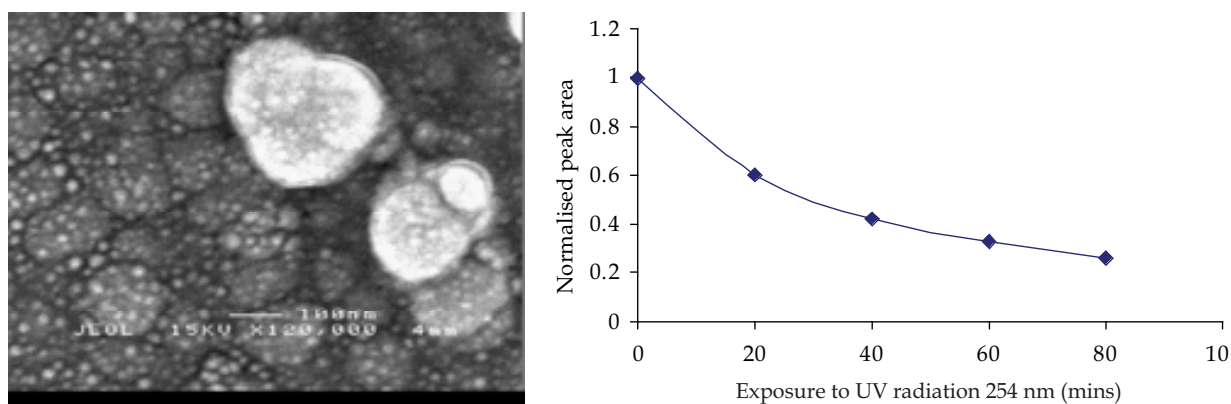


Fig. 6. (Left) SEM image showing a compact background with nanoparticles of approximate diameter 12 nm along with larger ovals 100 nm wide. (Right) Decrease in stearic acid C-H peak area for a ceria-titania film prepared by AACVD at  $500^\circ\text{C}$  upon radiation with UV light (Quershi et al. 2009).

The nanocomposite thin film showed promise both for photocatalysis (Figure 6) and as a super hydrophilic coating, although no significant increase in photocatalytic ability or reduction in contact angle of the composite film was reported compared to a plain titanium dioxide anatase thin film.

Walters et al. in their 2009 paper investigated the use of p-type dopants and noble metal dopants to influence the preferential orientation of ZnO thin films (Walters & Parkin 2009a). Films were prepared using AACVD from zinc acetylacetonate in water with one of the following as a nanoparticle source; auric acid, silver acetylacetonate, copper (II) acetylacetonate or aluminium nitrate. The choice of nanoparticle precursor fundamentally changed the morphology of the deposited nanocomposite film (figure 7).

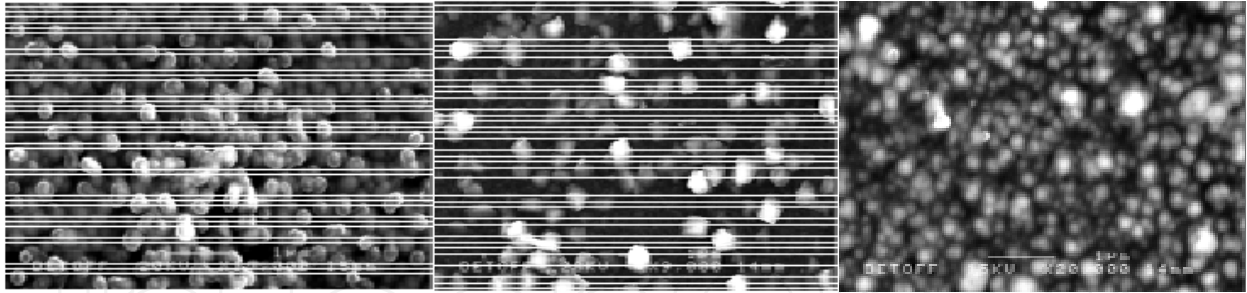


Fig. 7. SEM morphology of Ag Doped ZnO thin film Al ( $\text{Al}_2\text{O}_3$ ) doped ZnO thin Film ( $400^\circ\text{C}$ ) of Cu ( $\text{CuO}/\text{Cu}_2\text{O}$ ) doped ZnO thin films (Walters & Parkin 2009a).

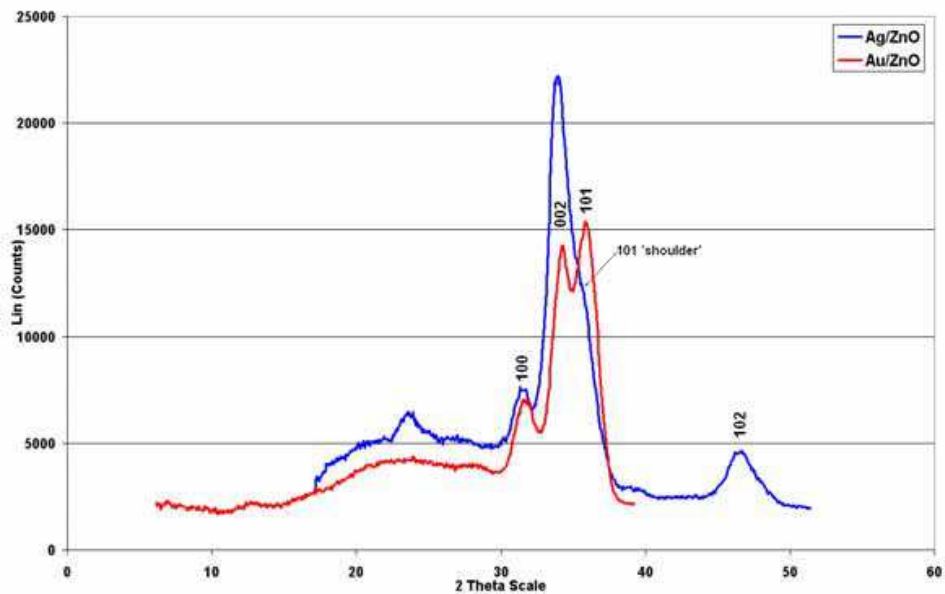
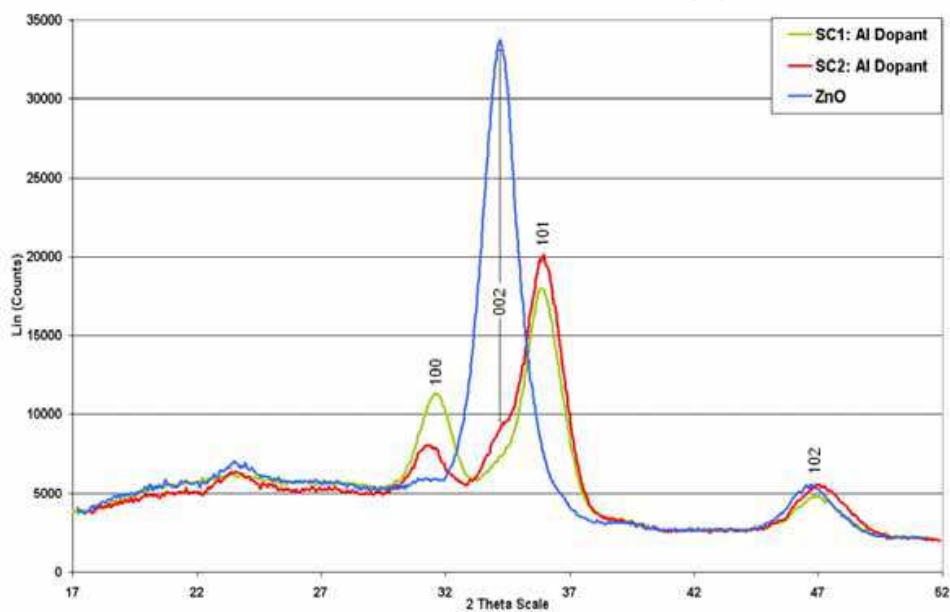


Fig. 7D. Comparison of XRD pattern for Al doped ZnO thin film and Undoped ZnO thin film c) XRD pattern for ZnO Au and Ag doped thin films (Walters & Parkin 2009a).

The authors report that the incorporation of aluminium oxide and copper oxide nanoparticles was much easier and likely to be due to the reaction of the copper and aluminium precursors on the surface of the growing film. In contrast the incorporation of gold and silver nanoparticles was difficult due to thermophoretic effects this suggests that nanoparticle formation of these materials occurs primarily in the gas phase. This is unsurprising as silver and gold are poorly oxophilic and thus are more inclined to form metal nanoparticles rather than bonding to surface oxygen sites on the growing film.

The incorporation of nanoparticles into the zinc oxide films led to significant changes in the preferred orientation of the deposited films (figure 7D). As deposited zinc oxide films showed a preference for a (002) orientation that has been reported as the most electrically conductive for zinc oxide, the incorporation of  $\text{Al}_2\text{O}_3$ , Au or Ag nanoparticles saw the preferred orientation change to the (101) direction, whilst the incorporation of copper appeared not to affect the film orientation.

Most recently Warwick et al. have investigated the use of AACVD for the production of multifunctional thin films. The authors deposited nanocomposite thin films where both the host matrix and guest nanoparticles had independent and well-established functional properties. Photocatalytic titanium dioxide was chosen for the host matrix and tin oxide for the guest nanoparticles. Tin oxide is well known for being infrared reflective and finds use in Low emissivity glazing (Warwick et al. 2010).

Precursor flasks were prepared with constant amounts of tin dioxide nanoparticles dispersed in methanol and varying levels of TTIP as the titanium precursor and varying levels of tin dioxide nanoparticles dispersed in methanol (Table 1). Scanning electron microscopy (figure 8.) indicated an island growth morphology. A typical island size of 300 nm and significant island agglomeration is observed for titanium dioxide films grown without any nanoparticles (figure 8A).

The incorporation of tin dioxide nanoparticles into the films (figure 8B & 8C) did not change the island size but affected the agglomerate size. As more nanoparticles were incorporated the agglomerate size increased from 400 nm for sample 4 (0.8 at. % nanoparticles) to 1,200 nm for sample 2 (Figure 8C, 3.0 at. % nanoparticles).

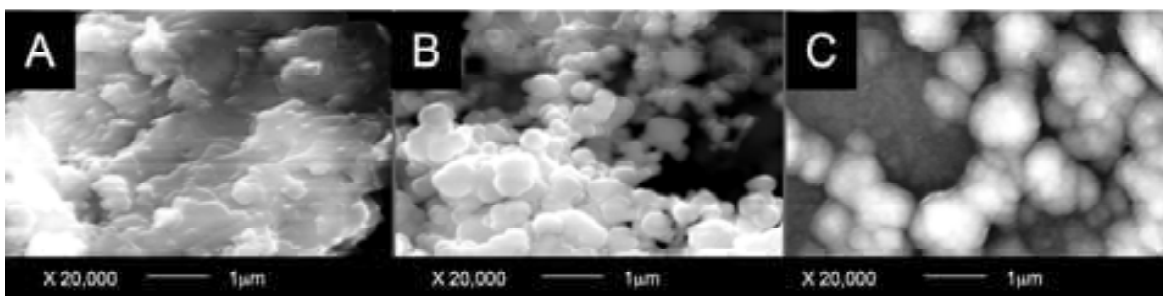


Fig. 8. Scanning electron microscope images of nanocomposite samples: A)  $\text{TiO}_2$ , B)  $\text{TiO}_2$  containing 1.8%  $\text{SnO}_2$  nanoparticles and C)  $\text{TiO}_2$  containing 3.0%  $\text{SnO}_2$  nanoparticles (Warwick et al. 2010).

Analysis with energy dispersive analysis of X-rays indicated that the films contained titanium, oxygen and tin (summarised in Table 1.) and no contaminant. X-ray photoelectron spectroscopy confirmed the presence of tin dioxide nanoparticles throughout the thickness of the nanocomposite film.

Sample	Volume of 0.05M Ti(OPr) <sub>4</sub> solution in reaction flask / ml	Volume of SnO <sub>2</sub> nanoparticle solution in reaction flask / ml	Phase as determined by EDAX/XRD [film thickness / nm]	Sn concentration as determined by EDAX & WDAX / at. %.
1	1	0 (25 ml of Toluene used)	Anatase TiO <sub>2</sub> [1050]	0
2	1	25	Anatase TiO <sub>2</sub> [980]	3.0
3	2	25	Anatase TiO <sub>2</sub> [990]	1.8
4	3	25	Anatase TiO <sub>2</sub> [1085]	0.9
5	4	25	Anatase TiO <sub>2</sub> [915]	0.8

Table 1. Table of experimental conditions and analytical results. All depositions were performed with a substrate temperature of 450 °C and a carrier gas flow rate of 1 l.min<sup>-1</sup>.

Photocatalysis is the primary functionality of the titanium dioxide film and methylene blue testing was carried out to gain information on the relative photo-catalytic abilities of the films. A plain titanium dioxide film performed the best and the inclusion of tin dioxide nanoparticles led to a minimal decrease in photo-catalytic ability, and not appear to correlate with the percentage of nanoparticles incorporated into the film. The reflectivity in the near infrared region (1500 – 2500 nm) was investigated using UV/Vis. The authors report that the reflectance of the films in this region increased with the incorporation of tin dioxide nanoparticles. This correlated with the percentage of nanoparticles incorporated in the film, with higher nanoparticle incorporation leading to higher infrared reflectance (Figure 9). The inclusion of 3 at. % tin oxide nanoparticles led to a reflectance at 2000 nm of 32 %. The inclusion of 1.8 at. % tin oxide nanoparticles caused a lower of reflectance at 2000 nm of 26 %. A plain titanium dioxide film showed a reflectance at 2000 nm of 17 %.

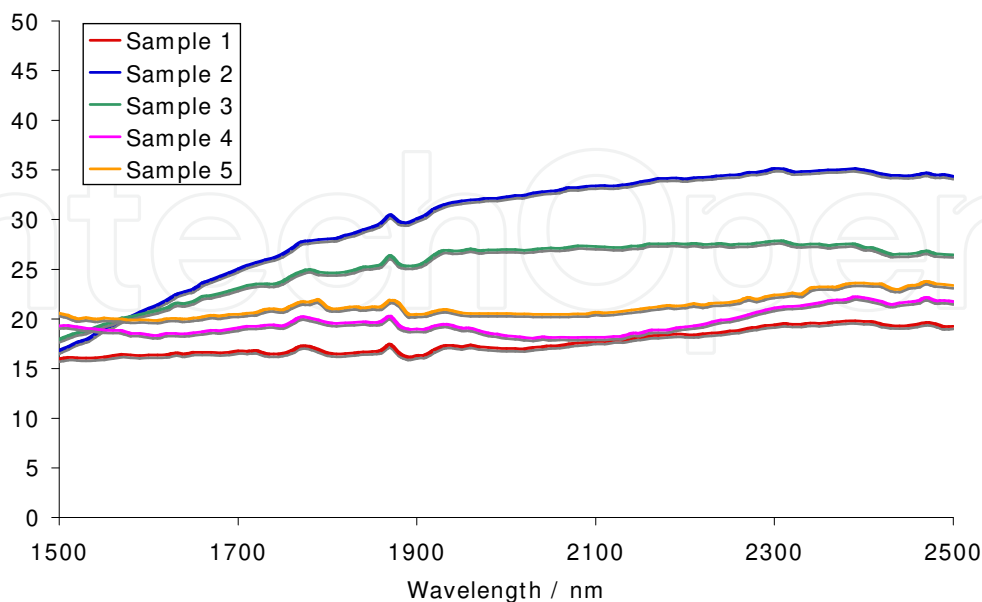


Fig. 9. Far infrared reflectance spectra of titanium dioxide tin dioxide nanocomposites (Warwick et al. 2010).

### 3. Hybrid chemical vapour deposition

#### 3.1 Introduction to hybrid CVD

Hybrid CVD combines atmospheric pressure CVD and aerosol assisted CVD. The technique was first developed by Binions (Binions 2009) as a method of combining unusual precursor species in a more traditional CVD setup whilst avoiding the potential pitfalls of aerosol based systems. AACVD is advantageous in that it allows the use of exotic precursor species, such as nanoparticle dispersions, but does not guarantee that adherent thin films will be produced from them. Indeed it has been observed in several papers that the use of certain precursors in AACVD leads to powdery and poorly adherent films (Binions et al. 2004).

A schematic setup of the hybrid CVD system is shown below in figure 10. The system combines a conventional APCVD setup with an aerosol inlet into the reaction chamber.

The first setup used by Binions added the aerosol mist into the plain line flow and this had to pass through the mixing chamber. This tended to cause blockages, as the APCVD precursors would often readily react with the aerosol solvent, leading to the deposition of metal oxide in the mixing chamber. The positioning of the aerosol inlet relative to the APCVD inlet has also proven to be crucial to obtaining good quality films. For the best quality films the aerosol inlet needs to be directly underneath the APCVD inlet, this ensures good mixing of the two flows, even distribution of nanoparticles through out the deposited film and a suppression of thermophoretic effects. If the inlet is placed in another position then thermophoresis of the aerosol droplets can be a problem and as a consequence there is poor distribution of nanoparticles in the resultant film and significant deposition on the reactor top plate rather than the desired substrate.

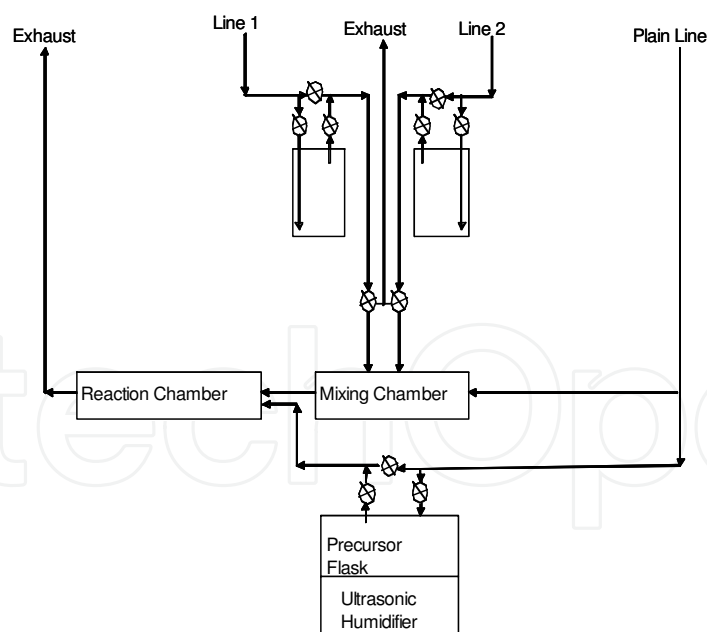


Fig. 10. Schematic of hybrid aerosol assisted and atmospheric pressure chemical vapour deposition rig (Binions 2009).

#### 3.2 Hybrid CVD of nanocomposites

Hybrid CVD has been used to deposit a variety of thermochromic nanocomposite thin films in an effort to improve the potential energy saving affect that a thermochromic coating may

have in an intelligent glazing system. Thermochromic thin films (figure 11) have been postulated as useful in glazing for some time (Binions & Kanu 2010) as above a certain (tunable) temperature the film becomes reflective to incoming infrared solar radiation reducing the amount of solar heat gain in the building and reducing the need for air conditioning. At lower temperatures solar heat gain is maximised and there is less need for heating.

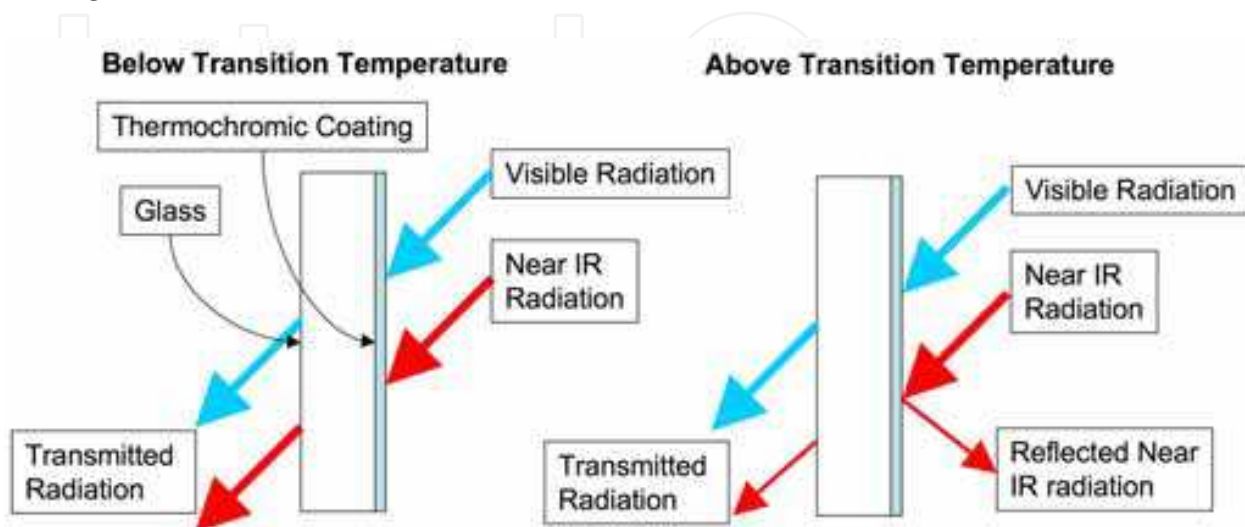


Fig. 11. Schematic of the application of thermochromic materials to advanced window glazing

Current approaches use static systems, with invariant properties, such as always infrared reflective. However, such systems are less suitable for variable climates such as those found in the UK or USA as they either minimise solar heat gain causing a need for extra heating in winter or maximise solar heat gain causing a need for extra cooling in summer. Thermochromic coatings theoretically maximise heat gain in winter and minimise heat gain in summer. Currently thermochromic thin films are not commercially available.

Composite  $\text{VO}_2$  / Au nanoparticle films were grown by the use of hybrid aerosol assisted / atmospheric pressure CVD from  $[\text{HAuCl}_4]$  and tetraoctylammonium bromide (TOAB) in methanol (the aerosol component) and  $[\text{VO}(\text{acac})_2]$  (the atmospheric pressure component). The films showed good surface coverage, uniformity and reproducibility. Increasing or decreasing the time of deposition could easily vary film thickness. In all cases at least the first 75% of the substrate is covered, similar to that observed previously with  $\text{VO}_2$  films produced from the APCVD reaction of vanadyl acetylacetonate and with other APCVD systems. Similarly there are changes in thickness that correlate with the temperature gradient across the substrate surface as seen previously (Binions et al. 2007) and a highly uniform area 2 cm x 5 cm in the middle of the substrate.

Secondary electron imaging (Figure 12A) indicates the formation of rod like crystallites of  $\text{VO}_2$  around 100 nm in width and up to 1.5  $\mu\text{m}$  long on the surface of the substrate, similar to morphologies previously seen in samples from the APCVD reaction of vanadyl acetylacetonate (Binions et al. 2007). Backscattered electron images (Figure 12B) indicate that gold is widely dispersed amongst the crystallites on the surface, rather than segregating as independent gold crystallites as has been observed with other methodologies, notably sol gel (Béteille et al. 1997).

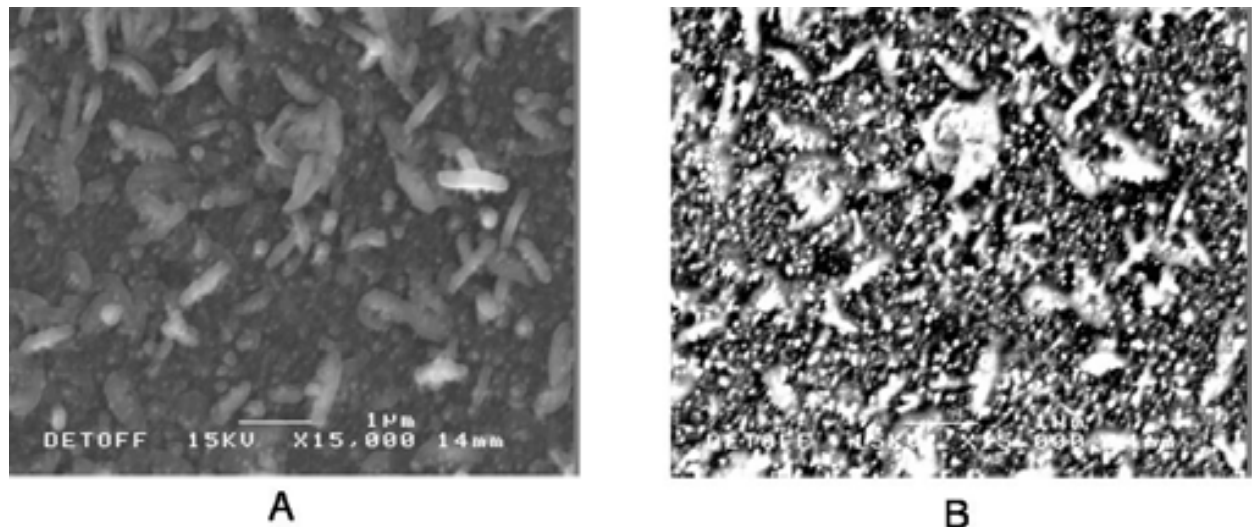


Fig. 12. A) Secondary electron image and B) Back scattered electron image of a sample typical of these gold doped vanadium dioxide sample deposited using the combined system over 15 minutes at a temperature of 525 °C (Binions et al. 2008)

Analysis with energy dispersive analysis of X-rays indicated that the films contained vanadium and gold and no contaminant, at least to the limit of detection of the EDAX methodology (around ½ atom % depending on the element). The amount of gold in the film was proportional to the ratio of the precursor flows.

In some circumstances TOAB was added to the reaction mixture in order to improve the particle size distribution. Scanning electron microscopy (Figure 13.) of these films indicated an island growth morphology. Typically for samples produced with TOAB a smaller average island size of 75 nm (Figure 13A) is seen compared with 150 nm (Figure 13B) for those produced without.

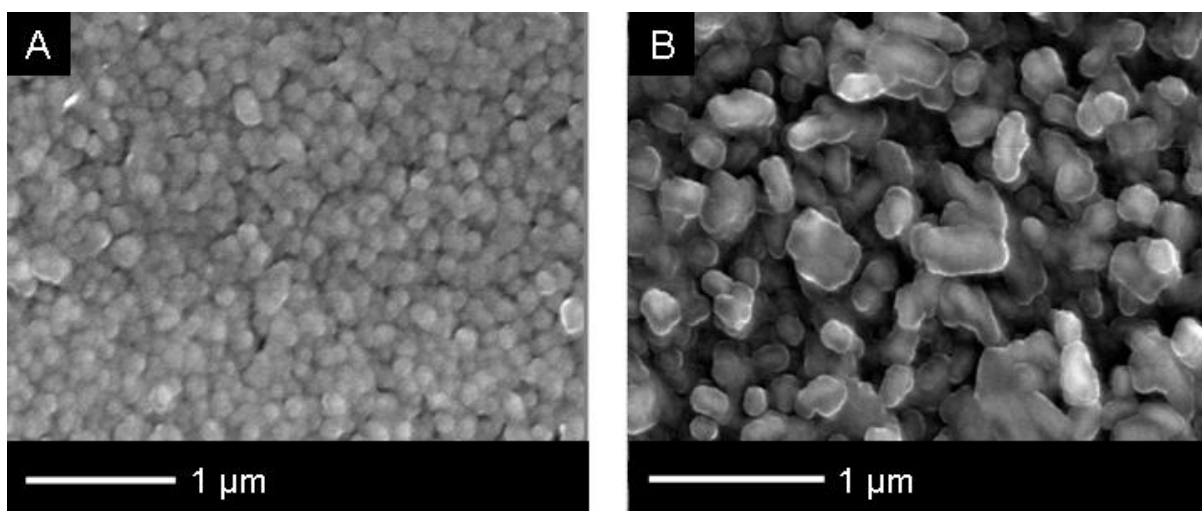


Fig. 13. Secondary electron scanning electron microscopy pictures of typical samples of a VO<sub>2</sub> / Au nanoparticle film produced using the hybrid AA/AP CVD methodology grown (A) with TOAB (B) without TOAB (Saeli et al. 2009a).

Backscattered electron imaging of films produced with TOAB and EDAX spot analysis indicated that gold is found amongst the crystallites on the surface. There were stark

differences between the gold crystallites grown with TOAB (Figure 14A) and those grown without (Figure 14B). The gold crystallites in films grown with TOAB formed spherical agglomerates with a diameter in the region of  $70 \pm 10$  nm. The gold crystallites in films grown without TOAB were very different; the crystallite agglomerates were smaller, around 40 nm diameter, and highly interconnected with no particular shape.

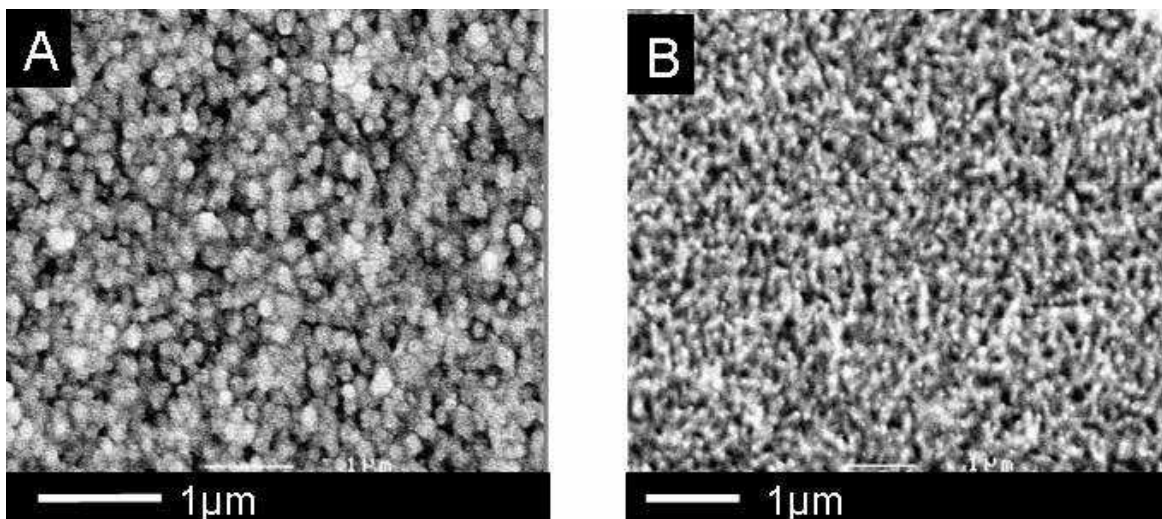


Fig. 14. Back scattered secondary electron scanning electron microscopy of typical samples of a  $\text{VO}_2$  / Au nanoparticle film produced using the hybrid AA/AP CVD methodology grown (A) with TOAB (B) without TOAB (Saeli et al. 2009a).

The microstructure of the films is significantly altered due to the use of TOAB in the reaction; in depositions without TOAB the island size of vanadium dioxide particles is around 150 nm and there is significant interconnectivity between agglomerates (Figure 13B), similar to that previously seen, whilst with the use of TOAB the agglomerate size is reduced to 75 nm and leads to a more discreet, rounded morphology. A similar effect is seen when observing the gold nanoparticles in the films using backscattered electron imaging (Figure 14.). The films produced without TOAB show a variety of gold nanoparticle shapes and sizes, significant but random agglomeration and interconnectivity. The films produced using TOAB are very different, the gold nanoparticle agglomerates are uniform in shape and size (approximately 75 nm diameter spheres). This is due to a surfactant effect caused by the TOAB that has been seen previously (Saeli et al. 2009b). It is less expected that the use of TOAB would cause a change in the overall film morphology between films grown under otherwise identical conditions.

The colour of the films could be altered substantially with a range of blues and greens being produced in contrast to the yellow/brown colour normally associated with monoclinic vanadium dioxide; this is attributed to the inclusion of gold nano-particles in the  $\text{VO}_2$  matrix. UV/Vis absorbance spectroscopy of the gold doped films indicates that a plasmon resonance band is present; however this is very broad,  $\sim 100$  nm, due to significant variation of gold nano-particle size (Figure 15.). The strength of the band correlates strongly with the gold to vanadium ratio in the films. The addition of TOAB into the precursor flask also causes a significant shift in the SPR centre as the size of the nanoparticles becomes more clearly defined (Figure 15).

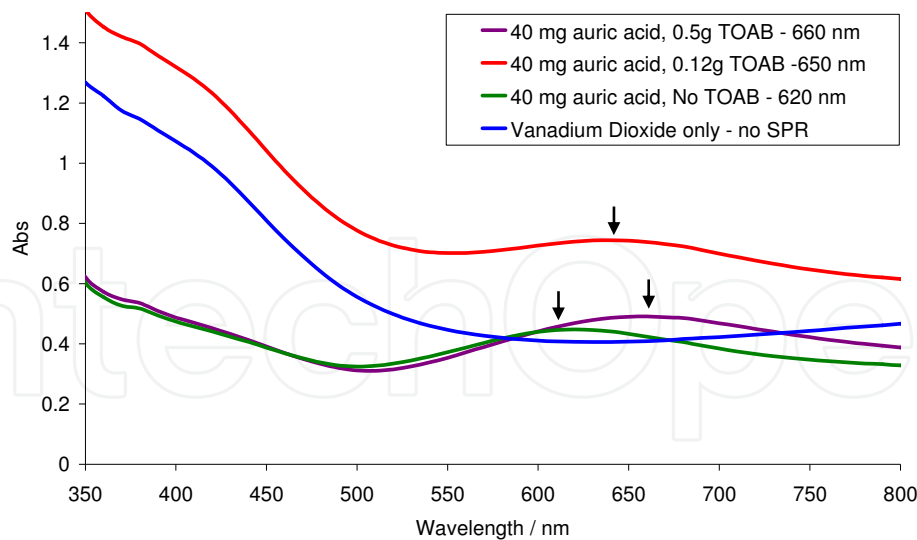


Fig. 15. UV/Vis spectroscopy and surface plasmon centres of typical samples of a  $\text{VO}_2$  / Au nanoparticle film produced using the hybrid AA/AP CVD methodology grown with TOAB and without TOAB. The arrows mark the position of the surface plasmon band resonance centre. The absorbance spectrum of a  $\text{VO}_2$  film is included for comparison (Saedi et al. 2009a).

X-ray diffraction analysis (Figure 16) indicated that in all cases cubic gold and monoclinic vanadium dioxide are formed. In some cases there is some evidence of the formation of  $\text{V}_2\text{O}_5$ . This is not entirely unexpected as X-ray photoelectron analysis of the sample surface suggests a variety of vanadium environments, we believe  $\text{V}_2\text{O}_5$  to be present only at the surface; indeed, on etching only a single vanadium environment is observed consistent with vanadium dioxide. Previous work on vanadium dioxide by APCVD has seen a similar phenomenon and has shown that surface  $\text{V}_2\text{O}_5$  does not affect the thermochromic behaviour of the bulk film (Binions et al. 2007). XPS shows that the gold is found in a single metallic environment, this indicates several things: There are no other detectable gold compounds present in the film, there is no un-reacted precursor on the film surface and indicates that the gold is present only as gold nanoparticles on the surface and in the bulk of the host film matrix. XPS and Raman spectroscopy were used to evaluate carbon contamination in the films; carbon could not be detected in the bulk of the films using these methods, some carbon was detected on the surface of the films using XPS but is most likely from an external source.

All of the films show thermochromic behaviour with reduced transition temperatures. Typically the hysteresis width of gold doped vanadium dioxide thin films is quite wide in the range of 15 – 20 °C compared to 10 °C as seen with some tungsten doped samples produced by APCVD and 10 – 15 °C seen for films produced by Sol-Gel methodology (Béteille & Livage 1998). The hysteresis width seemed not to matter on the amount of gold present in the film. Ideally this hysteresis would be as thin as possible to maximise the energy saving effect. The hysteresis width is attributable to several factors such as a variety of grain size and or crystallographic orientation (Binions et al. 2007). Indeed the transition temperature is reduced to ~50 °C, which is independent of the amount of gold in the films. It is likely that this reduction is caused by strain as a result of preferential orientation as observed previously, indeed the X-ray diffraction pattern has only one significant observable peak, the 011, suggesting a high degree of preferred orientation. It was not possible to perform a meaningful Reitveld analysis as we are only able to observe two

peaks, two smaller peaks in the VO<sub>2</sub>(m) diffraction pattern are obscured by the peaks due to gold. Similarly films that were prepared by sol gel gave transition temperatures of ~55 °C similar to un-doped films prepared by the same method, indeed the X-ray diffraction patterns of these films have a very strong 011 reflection (Binions et al. 2007). By comparison samples of gold doped nano-composites produced by laser ablation and thin films prepared by reactive ion beam sputtering have transition temperatures similar to un-doped vanadium dioxide of around 68 °C, unfortunately no X-ray diffraction data is presented for comparison. As seen with un-doped and tungsten doped samples prepared by CVD a large change in transmission is observable at 2500 nm, typically 35-40% comparable with previous literature values (Binions et al. 2007). The reflectance spectrum is different there is only a small change of around 10% on undergoing the transition. This is attributable to the higher reflectance of the films below the transition temperature, due to the metallic nature of the gold nanoparticles. Un-doped or tungsten doped films of monoclinic vanadium dioxide do not have as significant a metallic contribution to the reflectance and the change at 2500 nm on undergoing the MST is around 35% (Binions et al. 2007).

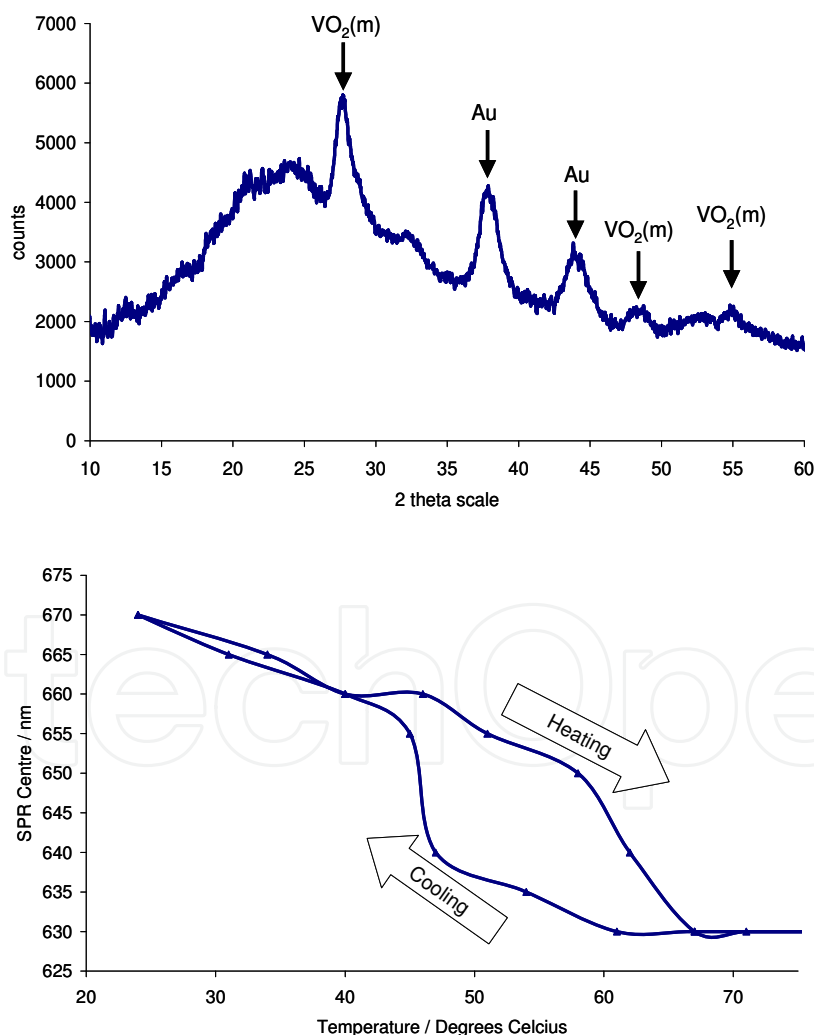


Fig. 16. (Left) X-ray diffraction pattern of typical Au/VO<sub>2</sub> nanocomposite grown using the hybrid methodology. (Right) Typical SPR hysteresis behaviour of gold-doped vanadium dioxide samples deposited using the hybrid methodology (Binions et al. 2008).

Figure 16 details the temperature dependent hysteresis of the surface plasmon resonance (SPR) band. The SPR band changes with temperature as the rutile and monoclinic forms of vanadium dioxide provide different dielectric environments. The SPR hysteresis behaviour is similar to the optical hysteresis – the hysteresis width is around 20 °C and it indicates a transition temperature of ~ 50 °C. In comparison to SPR hysteresis observed from gold doped vanadium dioxide nano-composites produced by laser ablation (Maaza et al. 2005) the hysteresis width is similar and there is a comparable change of SPR wavelength of 40 nm. The colour of the films (Figure 17) could be altered substantially with a range of blues and greens being produced in contrast to the yellow / brown colour normally associated with monoclinic vanadium dioxide; this is attributed to the inclusion of gold nanoparticles in the VO<sub>2</sub> matrix. The films became bluer in colour with the incorporation of more gold nanoparticles in the films.

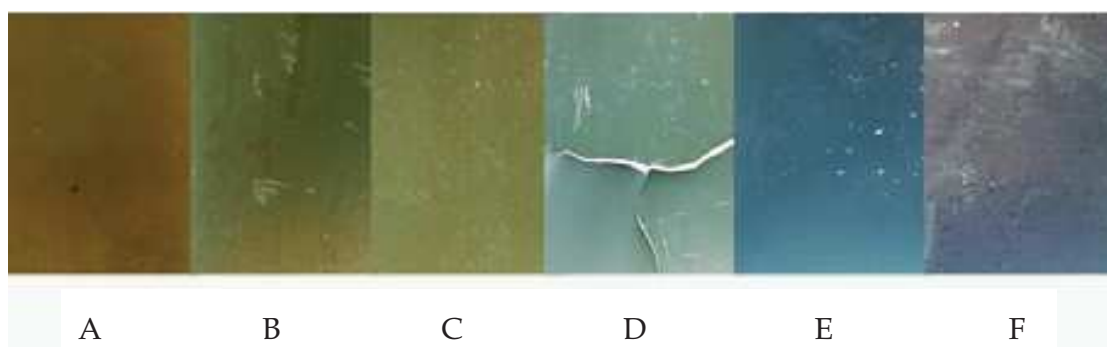


Fig. 17. Examples of glass (3 x 5 cm approximate size) with gold and vanadium dioxide nanocomposite films. The films had a V/Au ratio determined by EDAX of: A) 0 (W doped VO<sub>2</sub>) B) 0.09 C) 0.15 D) 0.30 E) 0.36 F) ∞ (gold nanoparticle film) (Saeli et al. 2010).

The experimental routes and characterisation of the thermochromic thin films used in this study have been reported previously (Saeli et al. 2010). We have used four different types of thermochromic film in our modelling: pure vanadium dioxide, vanadium dioxide with gold nanoparticles, pure vanadium dioxide grown with a growth directing surfactant, and vanadium dioxide grown with both a growth directing surfactant and gold nanoparticles. These are compared with three standard commercial products, as summarised in table.

The thermochromic coatings were deposited onto Optifloat clear (plain float glass) 4 mm thick glass. Spectral data was recorded using a Perkin Elmer Lambda 950 spectrophotometer. Emissivity data was obtained using a Perkin Elmer PE883 dual-beam IR spectrophotometer, using a NPL calibrated IR mirror as the reference standard. Emissivity was calculated according to standard EN763.

Energy Plus software developed by the Lawrence Berkeley National Laboratory and US Department of Energy was used to perform energy simulations and analysis. Energy Plus™ is an energy analysis and thermal load simulation program. Based on a user's description of a building from the perspective of the building's physical make-up, associated mechanical systems etc.

A series of simulations with different configurations and settings were run in order to evaluate the performance of the thermochromic coatings in different climates. The simulation set period is one year, with data points gathered every hour.

A very simple model of a room in a building was constructed in Energy Plus™. The room has external dimensions 6 x 5 x 3 m (length x width x height) and it is placed so that the axis

of every wall is perpendicular to one of the orientation North, South, West and East. We consider the room to represent the façade of a generic building so that just one wall is exposed to the external environment (weather, sun, wind, etc.); the remaining three walls are not affected by external conditions. The building is located in the northern hemisphere and the external wall is supposed to be exposed to the southern side.

Two different glazing possibilities were considered; one where the window was 1.5 x 2.5 m located in the middle of the southern wall surface (covering 25% of this surface) considered to represent a residential scenario. The other comprised the whole of the southern face (100%) – a glazing wall, representing a modern commercial building.

Further details governing the materials used for walls etc, have been previously reported (Saeli et al. 2010). In both cases the window is double glazed with a 12 mm air cavity, the coating was always modelled on the inside face of the outer pane. The only difference between each simulation was the glazing or coating used, the 7 examples investigated are summarised in table 2.

Sample	T <sub>c</sub> / °C	Cold Visible Transmittance/%	Hot Visible Transmittance/%	Room Temperature Emissivity	Hot State Emissivity
Optifloat Clear (plain float glass)	-	92	92	0.837	0.837
Sputtered Silver Coated Glass (thin metallic coating - SB)	-	82	82	0.030	0.030
Blue Body Tinted Glass (body tinted absorbing glass - AB)	-	76	76	0.837	0.837
Thermochromic 1 (VO <sub>2</sub> )	59	78	74	0.825	0.795
Thermochromic 2 (VO <sub>2</sub> + Gold)	43	56	48	0.800	0.752
Thermochromic 3 (VO <sub>2</sub> + TOAB)	38.5	61	51	0.827	0.789
Thermochromic 4 (VO <sub>2</sub> + Gold + TOAB)	45.5	77	49	0.828	0.797

Table 2. Summary of coatings, glass and optical data examined in this study

The external ground temperatures were taken to be 18 °C throughout the year, as this remains relatively constant after a small depth. The internal conditions were chosen to be air-conditioned between 19 – 26 °C to maintain a comfortable working/living environment. The required illuminance level in an office building is taken to be 500 lux, this corresponds to a lighting load of 400 W. The lights are fully dimmable: lowering their output when there is an adequate illuminance from the sun, in order to save energy. It is considered that they can be dimmed in the whole range from 0 to 100 %. The dimming control is automatic and zoned. The casual heat gain (persons + equipment) is taken to be 500 W in total and the ventilation rate used is 0.025 m<sup>3</sup>/s. Building occupancy was set as occupied from 8:00 till

18:00, five days a week, as is normal for an office. The simulations were run for a number of different cities in Europe and one in northern Africa in order that a wide range of climatic conditions were covered. The specific cities chosen for the simulations were: Cairo (Egypt), Palermo, Rome and Milan (Italy), Paris (France), London (UK), Helsinki (Finland) and Moscow (Russia).

The model is clearly limited because the building is not ideal for all climates. Insulation layers, as well as the materials chosen here, in warmer and cooler climates would be different from that used in the model depending not only on local climate conditions but also on the constructive techniques and materials available in loco. Likewise the assumption that a constant ground temperature of 18 °C throughout the year is significant. However, by using the results obtained from the plain glass (Optifloat) simulations as a baseline we aim to isolate the change in energy performance caused by the use of different glazings.

The thermochromic properties of the glazing were modelled in version 3.0.0 of Energy Plus by entering the spectral data of the glazing in the hot and cold states. The glazing was switched between the hot and cold states using the shading control feature of EnergyPlus which can “replace” glazing elements in a window, according to environment conditions or set control criteria. The surface temperature of the glazing was correlated against incident solar radiation. The shading control automatically switched the glazing from the cold to hot state when the incident solar radiation exceeded that required for the glazing surface to exceed the transition temperature, switching back to the cold state when solar radiation fell below the trigger value.

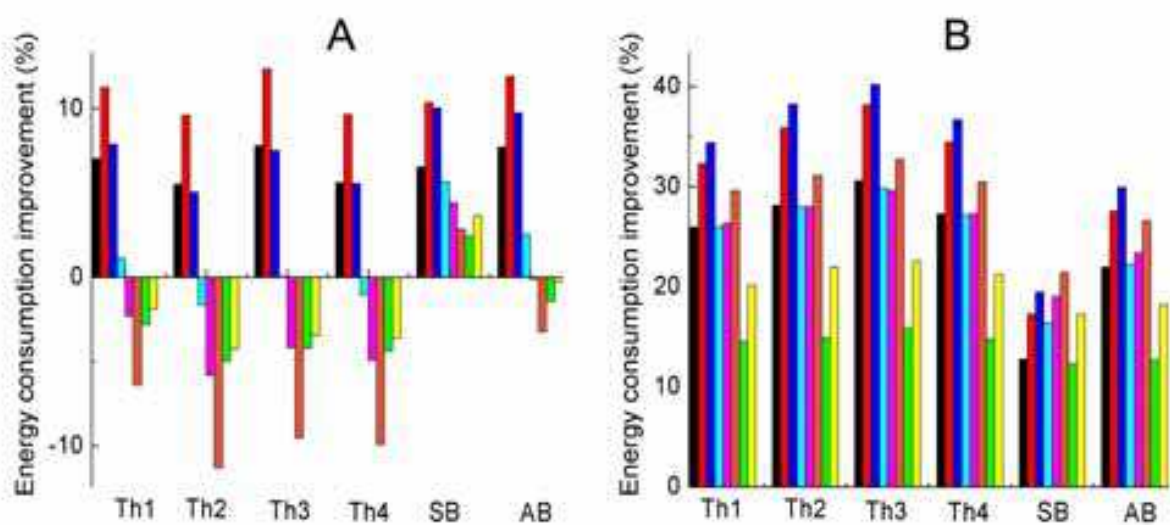


Fig. 18. (a) Total annual energy consumption and (b) percentage improvement to clear-clear glazing for the 100 % window to wall ratio model;

■ Cairo, ■ Palermo, ■ Rome, ■ Milan, ■ Paris, ■ London, ■ Moscow, ■ Helsinki.

The total energy consumption improvement for our building is taken as the sum of heating, cooling and artificial lighting energy required for the whole year period compared with a plain double glazed system, these results are presented in figure 18.

The total energy improvement is lower in the coldest cities. This can be explained by the low average temperatures, not allowing the thermochromic glazing to switch for significant periods of time into the hot state. As the thermochromic coatings display insignificant low-e

behaviour (table 2), we would not expect this sort of glazing to be suitable for colder climates. This is illustrated clearly in figure B where the overall performance in cooler climates is not as good as plain float glass.

In warmer climates however the thermochromic glazings perform more favourably than both plain glass and the commercial glazings evaluated here. The best behaviour is shown for thermochromic 3 in the city of Palermo for the 25% window model and in the city of Rome for the 100% window model.

The best overall performance is shown in the 100% window model in cities with warm climates. The thermochromic coatings are a more favourable choice for large glazed areas in these cities. Large glazed surfaces, such as the 100% window analyzed in this work, contribute to a greater percentage to the overall energy balance of the building, potentially minimizing heat losses and as in this case, controlling the incoming solar radiation.

It is interesting to note that the thermochromic 1 glazing, even though it never switches in its hot state because of its high switching temperature, still performs well in the warmer environmental conditions, albeit not as well as the other thermochromic coatings. This suggests that the variable heat mirror properties of thermochromic coatings are not the only important features of these coatings for solar control.

### 3.3 Use of preformed nanoparticles in hybrid CVD

Nanocomposite thin films of vanadium dioxide and either cerium dioxide or titanium dioxide nanoparticles were deposited using the hybrid AA/APCVD method from vanadyl acetylacetonate and an aerosol of nanoparticles at temperatures between 500 and 600 °C. The deposited films were brown in colour and showed significant surface coverage comparable to that seen previously using this method with vanadyl acetylacetonate [ref]. Compositional analysis of the films performed by EDAX indicated that the films contained vanadium, oxygen in an approximately 1:2 ratio and small amounts of cerium or titanium depending on the nanoparticle solution used. EDAX did not detect any contaminants at least to the limit of detection of this methodology (~1/2 atm%). Experimental conditions and compositional analysis are summarised in table 1. Analysis of film thickness indicated that the films were  $850 \pm 50$  nm thick, suggesting a nominal growth rate of  $42.5 \pm 2.5$  nm.min<sup>-1</sup>. (Binions et al 2007)

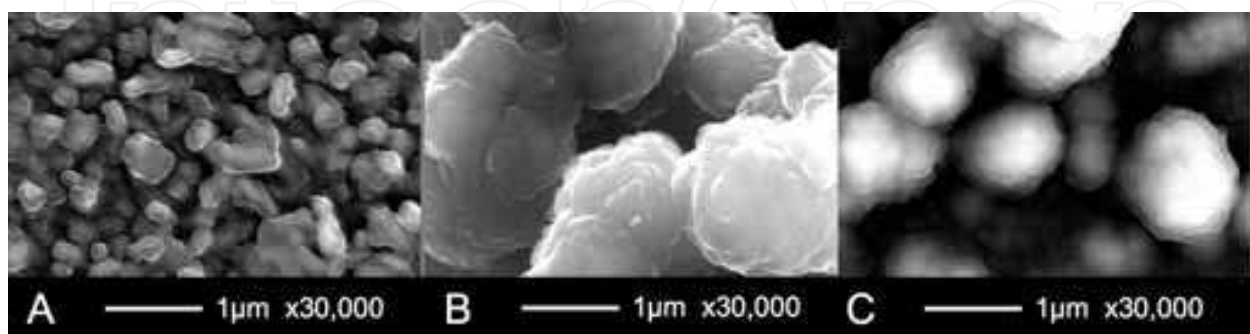


Fig. 19. Scanning electron microscope images of nanocomposite thin films samples produced using hybrid CVD.

Scanning electron microscopy of the samples (Figure 19) indicated that the films were formed of large agglomerates. The films made with titanium dioxide nanoparticles (Figure

19B) had agglomerates of 1 to 2  $\mu\text{m}$  in diameter, which are composed of smaller globules of material up to 300 nm in diameter. The films grown with cerium dioxide nanoparticles (Figure 19C) are similar being composed of agglomerates 800 nm to 1  $\mu\text{m}$  in diameter, again these are formed of smaller globules of material up to 300 nm in diameter. In both cases, backscattered electron imaging failed to distinguish the nanoparticles from the vanadium dioxide matrix. In the case of the films grown with the titanium dioxide nanoparticles, this is unsurprising as titanium and vanadium have similar atomic weights and we would not expect to see significant contrast between them. However, in the case of the films grown with cerium dioxide nanoparticles we also cannot detect significant contrast suggesting that the cerium dioxide nanoparticles are highly dispersed through out the vanadium dioxide matrix.

All of the films show thermochromic behaviour with reduced transition temperatures compared to undoped  $\text{VO}_2$  single crystals (typically 66 - 68  $^\circ\text{C}$ ) but are similar to un-doped  $\text{VO}_2$  thin films (50 - 66  $^\circ\text{C}$  depending on the growth conditions) (Binions et al. 2007). Typically, the hysteresis width of nanocomposite vanadium dioxide thin films is in the range of 15 - 20  $^\circ\text{C}$ . Only a small change in transmission is observable at 2500 nm (Figure 20), this is attributed to the thickness of the films. However the reflectance spectrum of the sample (Figure 20) shows a large change of 30 % on undergoing the transition, much larger than is usually observed and is again attributable to the film thickness (Binions et al. 2007).

Methylene blue photodecolourisation experiments were used to gain information on the relative photocatalytic activities of the films. Figure 20 shows the results of these experiments. In all cases, the samples showed better photocatalytic activity than plain untreated glass. The control samples of pure glass and vanadium oxide (sample 1) showed little or no decolourisation of the methylene blue. The pure anatase thin film showed a slow decay over the first 90 minutes (rate =  $7.8 \times 10^{13}$  molecules.min<sup>-1</sup>), which plateaued thereafter. The inclusion of either titanium dioxide or cerium dioxide nanoparticles into a vanadium dioxide matrix led to a significant increase in photocatalytic activity relative to a sample of pure vanadium dioxide, this does not appear to correlate strongly with the percentage of nanoparticles incorporated into the film. Photocatalytic activity was comparable to that of a film of anatase titanium dioxide prepared by AACVD (Warwick et al. 2010). This suggests that the reactions are limited by the low surface area of the coatings, however, a clear difference between active and inactive coatings can be observed based on initial decolourisation profiles.

Unexpectedly the incorporation of a larger percentage of photocatalytically active nanoparticles did not improve the photocatalytic activity of the films (Figure 20). We attribute this to the fact that film microstructure does not appreciably change with the incorporation of different amounts of nanoparticles in the aerosol portion of the hybrid flow (Figure 20). As nanoparticles are incorporated the films become composed of larger islands, as more nanoparticles are incorporated there is little affect on the film microstructure. Therefore the surface area of the films are likely to remain constant; so even though we would expect a higher number of nanoparticles incorporated to lead to a higher photocatalytic activity this is not the case. A larger proportion of nanoparticles must reside in the bulk of the film rather than at the surface of the film and are unable to influence the photocatalytic activity of the film.

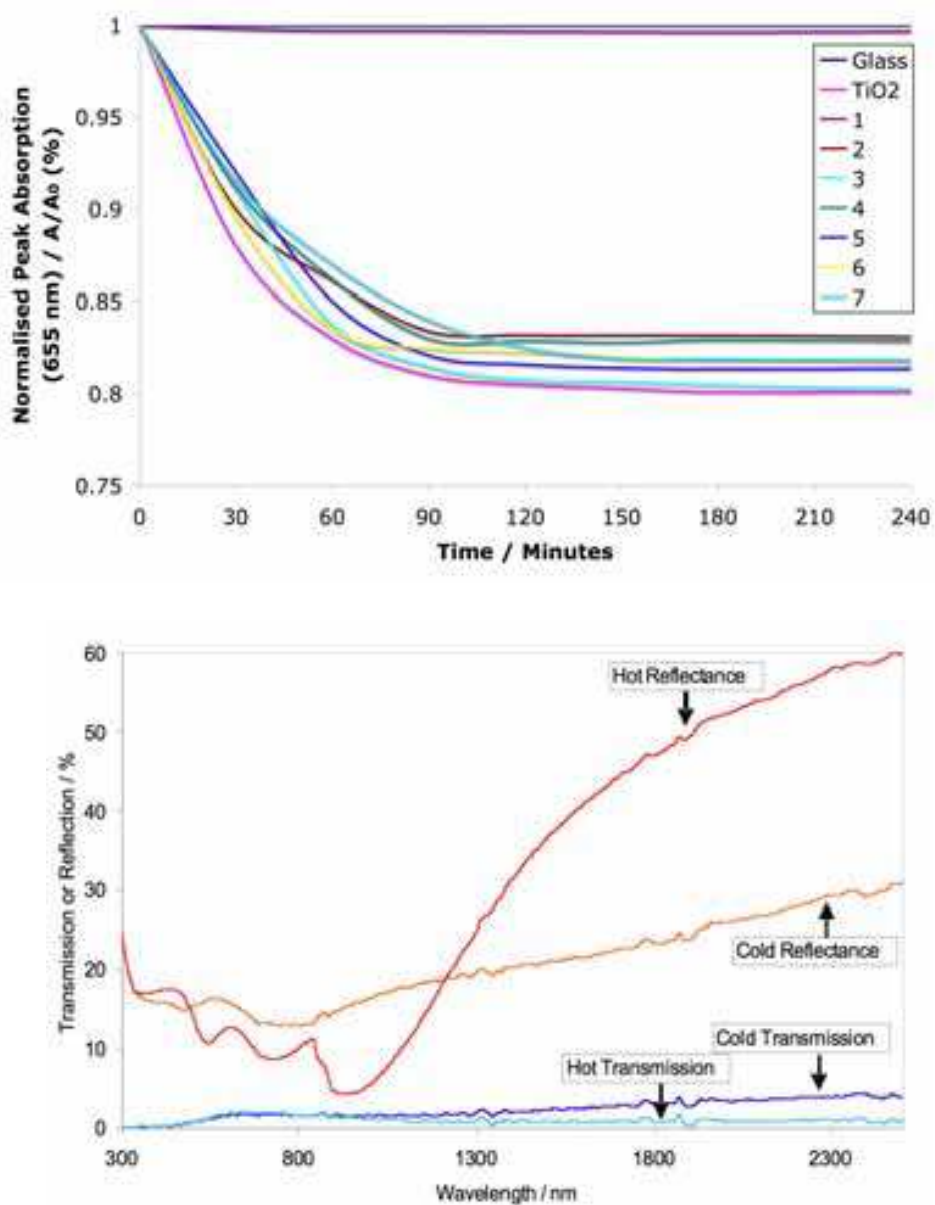


Fig. 20. (a) Methylene blue photocatalysis results and (b) variable temperature optical spectra for nanocomposite thin film samples prepared with preformed nanoparticles using the hybrid methodology.

#### 4. Conclusions and outlook

In this chapter we have demonstrated that several new and important CVD techniques are available for the production of nanocomposite thin film materials. We have shown that these methodologies can be used in one step experiments and incorporate preformed nanoparticle solutions or dispersions. The focus of our work has been on architecturally important materials and we have shown that it is possible to synthesise multifunctional films with enhanced properties; although in principle, any combination of matrix material and nanoparticles could be used to produce a wide array of exotic multifunctional nanocomposite thin films. Perhaps more importantly these methods are generally

applicable; CVD is already widely used in the glazing and microelectronics industries this approach could be easily integrated into the production of useful products and devices.

## 5. References

- Béteille, F. & Livage, J. 1998 Optical Switching in VO<sub>2</sub> Thin Films. *Journal of Sol-Gel Science and Technology* 13, 915-921.
- Béteille, F., Morineau, R., Livage, J. & Nagano, M. 1997 Switching properties of V<sub>1-x</sub>Ti<sub>x</sub>O<sub>2</sub> thin films deposited from alkoxides. *Materials Research Bulletin* 32, 1109.
- Binions, R. 2009 *Chemical Vapour Deposition of Main Group Metal Oxides and Phosphides: Aspects of Synthesis and Functional Property*. Saarbrücken: VDM Verlag Dr Muller.
- Binions, R., Carmalt, C. J. & Parkin, I. P. 2004 Aerosol-assisted chemical vapour deposition of sodium fluoride thin films. *Thin Solid Films* 469-470, 416.
- Binions, R., Hyett, G., Piccirillo, C. & Parkin, I. P. 2007 Doped and un-doped vanadium dioxide thin films prepared by atmospheric pressure chemical vapour deposition from vanadyl acetylacetonate and tungsten hexachloride: the effects of thickness and crystallographic orientation on thermochromic properties. *Journal of Materials Chemistry* 17, 4652-4660.
- Binions, R. & Kanu, S. S. 2010 Thin films for solar control applications. *Proceedings of the Royal Society of London. Series A. Mathematical and Physical Sciences* 466, 19-44.
- Binions, R., Piccirillo, C., Palgrave, R. G. & Parkin, I. P. 2008 Hybrid Aerosol Assisted and Atmospheric Pressure CVD of Gold-Doped Vanadium Dioxide. *Chemical Vapor Deposition* 14, 33-39.
- Blackman, C. S., Carmalt, C. J., Parkin, I. P., O'Neill, S. A., Molloy, K. C. & Apostolico, L. 2003 Chemical vapour deposition of crystalline thin films of tantalum phosphide. *Materials Letters* 57, 2634-2636.
- Blackman, C. S. & Parkin, I. P. 2005 Atmospheric pressure chemical vapor deposition of crystalline monoclinic WO<sub>3</sub> and WO<sub>3-x</sub> thin films from reaction of WCl<sub>6</sub> with O-containing solvents and their photochromic and electrochromic properties. *Chemistry of Materials* 17, 1583-1590.
- Choy, K. L. & Hou, X. 2008 Synthesis of Cr<sub>2</sub>O<sub>3</sub> based nanocomposite coatings with incorporation of inorganic fullerene like nanoparticles. *Thin Solid Films* 516, 8620-8624.
- Cross, W. B. & Parkin, I. P. 2003 Aerosol assisted chemical vapour deposition of tungsten oxide films from polyoxotungstate precursors: active photocatalysts. *Chemical Communications*, 1696-1697.
- Frey, K., Beck, A., Peto, G. b., Moln r, G., Geszti, O. & Guzzi, L. s. 2006 Activity of TiO<sub>2</sub> overlayer deposited on Au/SiO<sub>2</sub>/Si(100) model system. *Catalysis Communications* 7, 64-67.
- Green, M. 2005 Organometallic based strategies for metal nanocrystal synthesis. *Chemical Communications*, 3002-3011.
- Gyorgy, E., Sauthier, G., Figueras, A., Giannoudakos, A., Kompitsas, M. & Mihailescu, I. N. 2006 Growth of Au--TiO<sub>2</sub> nanocomposite thin films by a dual-laser, dual-target system. *Journal of Applied Physics* 100, 114302-5.
- Hampden-Smith, M. & Kodas, T. T. 1999 *Aerosol Processing of Materials*: Wiley-VCH.

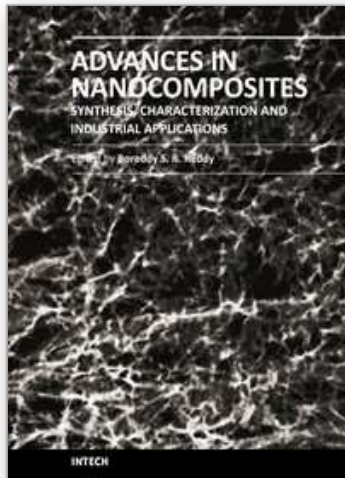
- Hida, Y. & Kozuka, H. 2005 Photoanodic properties of sol-gel-derived iron oxide thin films with embedded gold nanoparticles: effects of polyvinylpyrrolidone in coating solutions. *Thin Solid Films* 476, 264-271.
- Hitchman, M. L. & Jensen, K. F. 1993 *Chemical Vapour Deposition Principles and Applications*. London: Academic Press.
- Houng, B. & Huang, C.-J. 2006 Structure and properties of Ag embedded aluminum doped ZnO nanocomposite thin films prepared through a sol-gel process. *Surface and Coatings Technology* 201, 3188-3192.
- Jain, P., Huang, X., El-Sayed, I. & El-Sayed, M. 2007 Review of Some Interesting Surface Plasmon Resonance-enhanced Properties of Noble Metal Nanoparticles and Their Applications to Biosystems. *Plasmonics* 2, 107-118.
- Jones, A. C. & Hitchman, M. L. (ed.) 2009 *Chemical Vapour Deposition: Precursors, Processes and Applications*. Cambridge: RSC Publishing.
- Ko, H. Y. Y., Mizuhata, M., Kajinami, A. & Deki, S. 2005 The dispersion of Au nanoparticles in SiO<sub>2</sub>/TiO<sub>2</sub> layered films by the liquid phase deposition (LPD) method. *Thin Solid Films* 491, 86-90.
- Kuroda, N., Sugou, S., Koizumi, Y. & Uji, T. 1989 Epitaxial growth of highly Fe doped semiinsulating InP layers by N<sub>2</sub> carrier gas mixed hydride vapor phase epitaxy. *Journal of Crystal Growth* 96, 7-12.
- Liao, H., Wen, W. & Wong, G. K. 2006 Photoluminescence from Au nanoparticles embedded in Au:oxide composite films. *J Opt. Soc. Am. B* 23, 2518-2521.
- Maaza, M., Nemraoui, O., Sella, C. & Beye, A. C. 2005 Surface plasmon resonance tunability in Au-VO<sub>2</sub> nanocomposites. *Gold Bulletin* 38, 100-106.
- Manning, T. D., Parkin, I. P., Blackman, C. & Qureshi, U. 2005 APCVD of thermochromic vanadium dioxide thin films-solid solutions V<sub>2</sub>-MO<sub>2</sub> (M = Mo, Nb) or composites VO<sub>2</sub>: SnO<sub>2</sub>. *Journal of Materials Chemistry* 15, 4560-4566.
- Miao, G. X., Gupta, A., Xiao, G. & Anguelouch, A. 2005 Epitaxial growth of ruthenium dioxide films by chemical vapor deposition and its comparison with similarly grown chromium dioxide films. *Thin Solid Films* 478, 159-163.
- Michael L. Hitchman, K. F. J. 1993 *Chemical vapor deposition: principles and applications*, pp. 37.
- Mungkalasiri, J., Bedel, L., Emieux, F., Doré, J., Renaud, F. N. R. & Maury, F. 2009 DLI-CVD of TiO<sub>2</sub>-Cu antibacterial thin films: Growth and characterization. *Surface and Coatings Technology* 204, 887-892.
- Mungkalasiri, J., Bedel, L., Emieux, F., Doré, J., Renaud, F. N. R., Sarantopoulos, C. & Maury, F. 2010 CVD Elaboration of Nanostructured TiO<sub>2</sub>-Ag Thin Films with Efficient Antibacterial Properties. *Chemical Vapor Deposition* 16, 35-41.
- Palgrave, R. G. & Parkin, I. P. 2006 Aerosol Assisted Chemical Vapor Deposition Using Nanoparticle Precursors: A Route to Nanocomposite Thin Films. *Journal of the American Chemical Society* 128, 1587.
- Parkin, I. P., Binions, R., Piccirillo, C., Blackman, C. S. & Manning, T. D. 2008 Thermochromic Coatings for Intelligent Architectural Glazing. *Journal of Nano Research* 2, 1.
- Paul, R., Hussain, S., Majumder, S., Varma, S. & Pal, A. K. 2009 Surface plasmon characteristics of nanocrystalline gold/DLC composite films prepared by plasma CVD technique. *Materials Science and Engineering: B* 164, 156-164.

- Qureshi, U., Blackman, C., Hyett, G. & Parkin, I. P. 2007 Tungsten Oxide and Tungsten Oxide-Titania Thin Films Prepared by Aerosol-Assisted Deposition - Use of Preformed Solid Nanoparticles. *European Journal of Inorganic Chemistry* 2007, 1415-1421.
- Qureshi, U., Dunnill, C. W. & Parkin, I. P. 2009 Nanoparticulate cerium dioxide and cerium dioxide-titanium dioxide composite thin films on glass by aerosol assisted chemical vapour deposition. *Applied Surface Science* 256, 852-856.
- Qureshi, U., Manning, T. D., Blackman, C. & Parkin, I. P. 2006 Composite thermochromic thin films: (TiO<sub>2</sub>)-(VO<sub>2</sub>) prepared from titanium isopropoxide, VOCl<sub>3</sub> and water. *Polyhedron* 25, 334-338.
- Qureshi, U., Manning, T. D. & Parkin, I. P. 2004 Atmospheric pressure chemical vapour deposition of VO<sub>2</sub> and VO<sub>2</sub>/TiO<sub>2</sub> films from the reaction of VOCl<sub>3</sub>, TiCl<sub>4</sub> and water. *Journal of Materials Chemistry* 14, 1190-1194.
- Saeli, M., Binions, R., Piccirillo, C., Hyett, G. & Parkin, I. P. 2009a Templated growth of smart nanocomposite thin films: Hybrid aerosol assisted and atmospheric pressure chemical vapour deposition of vanadyl acetylacetonate, auric acid and tetraoctyl ammonium bromide. *Polyhedron* 28, 2233.
- Saeli, M., Binions, R., Piccirillo, C. & Parkin, I. P. 2009b Templated growth of smart coatings: Hybrid chemical vapour deposition of vanadyl acetylacetonate with tetraoctyl ammonium bromide. *Applied Surface Science* 255, 7291.
- Saeli, M., Piccirillo, C., Parkin, I. P., Ridley, I. & Binions, R. 2010 Nano-composite thermochromic thin films and their application in energy-efficient glazing. *Solar Energy Materials and Solar Cells* 94, 141-151.
- Serna, R. & et al. 2006 Optical evidence for reactive processes when embedding Cu nanoparticles in Al<sub>2</sub>O<sub>3</sub> by pulsed laser deposition. *Nanotechnology* 17, 4588.
- Shearer, J. C., Fisher, M. J., Hoogeland, D. & Fisher, E. R. 2010 Composite SiO<sub>2</sub>/TiO<sub>2</sub> and amine polymer/TiO<sub>2</sub> nanoparticles produced using plasma-enhanced chemical vapor deposition. *Applied Surface Science* 256, 2081-2091.
- Silva, M. F. t. V. & Nicholls, J. R. 2001 A model for calculating the thickness profile of TiB<sub>2</sub> and Al multilayer coatings produced by planar magnetron sputtering. *Surface and Coatings Technology* 142-144, 934-938.
- Tzu-Hsuan, K. & et al. 2006 Continuity and adhesion of Au deposits on electronic substrates by utilizing nanoparticle suspensions. *Nanotechnology* 17, 1416.
- Walters, G. & Parkin, I. P. 2009a Aerosol assisted chemical vapour deposition of ZnO films on glass with noble metal and p-type dopants; use of dopants to influence preferred orientation. *Applied Surface Science* 255, 6555-6560.
- Walters, G. & Parkin, I. P. 2009b The incorporation of noble metal nanoparticles into host matrix thin films: synthesis, characterisation and applications. *Journal of Materials Chemistry* 19, 574-590.
- Wang, D.-Y., Lin, H.-C. & Yen, C.-C. 2006 Influence of metal plasma ion implantation on photo-sensitivity of anatase TiO<sub>2</sub> thin films. *Thin Solid Films* 515, 1047-1052.
- Warwick, M. E., Dunnill, C. W. & Binions, R. 2010 Multifunctional Nanocomposite Thin Films by Aerosol-Assisted CVD. *Chemical Vapor Deposition* 16, 220-224.
- Yang, K., Fan, H., Malloy, K. J., Brinker, C. J. & Sigmon, T. W. 2005 Optical and electrical properties of self-assembled, ordered gold nanocrystal/silica thin films prepared by sol-gel processing. *Thin Solid Films* 491, 38-42.

- Zhang, W. J., Matsumoto, S., Li, Q., Bello, I. & Lee, S. T. 2002 Growth behavior of cubic boron nitride films in a two-step process: Changing bias voltage, gas composition, and substrate temperature. *Advanced Functional Materials* 12, 250-254.
- Zorica, K. & et al. 2006 Particle growth mechanisms in Ag,AlZrO<sub>2</sub> and AuAlZrO<sub>2</sub> granular films obtained by pulsed laser deposition. *Nanotechnology* 17, 4106.

IntechOpen

IntechOpen



## **Advances in Nanocomposites - Synthesis, Characterization and Industrial Applications**

Edited by Dr. Boreddy Reddy

ISBN 978-953-307-165-7

Hard cover, 966 pages

**Publisher** InTech

**Published online** 19, April, 2011

**Published in print edition** April, 2011

Advances in Nanocomposites - Synthesis, Characterization and Industrial Applications was conceived as a comprehensive reference volume on various aspects of functional nanocomposites for engineering technologies. The term functional nanocomposites signifies a wide area of polymer/material science and engineering, involving the design, synthesis and study of nanocomposites of increasing structural sophistication and complexity useful for a wide range of chemical, physicochemical and biological/biomedical processes. "Emerging technologies" are also broadly understood to include new technological developments, beginning at the forefront of conventional industrial practices and extending into anticipated and speculative industries of the future. The scope of the present book on nanocomposites and applications extends far beyond emerging technologies. This book presents 40 chapters organized in four parts systematically providing a wealth of new ideas in design, synthesis and study of sophisticated nanocomposite structures.

### **How to reference**

In order to correctly reference this scholarly work, feel free to copy and paste the following:

Russell Binions and Ivan P. Parkin (2011). Novel Chemical Vapour Deposition Routes to Nanocomposite Thin Films, Advances in Nanocomposites - Synthesis, Characterization and Industrial Applications, Dr. Boreddy Reddy (Ed.), ISBN: 978-953-307-165-7, InTech, Available from: <http://www.intechopen.com/books/advances-in-nanocomposites-synthesis-characterization-and-industrial-applications/novel-chemical-vapour-deposition-routes-to-nanocomposite-thin-films>

**INTECH**  
open science | open minds

### **InTech Europe**

University Campus STeP Ri  
Slavka Krautzeka 83/A  
51000 Rijeka, Croatia  
Phone: +385 (51) 770 447  
Fax: +385 (51) 686 166  
[www.intechopen.com](http://www.intechopen.com)

### **InTech China**

Unit 405, Office Block, Hotel Equatorial Shanghai  
No.65, Yan An Road (West), Shanghai, 200040, China  
中国上海市延安西路65号上海国际贵都大饭店办公楼405单元  
Phone: +86-21-62489820  
Fax: +86-21-62489821

© 2011 The Author(s). Licensee IntechOpen. This chapter is distributed under the terms of the [Creative Commons Attribution-NonCommercial-ShareAlike-3.0 License](#), which permits use, distribution and reproduction for non-commercial purposes, provided the original is properly cited and derivative works building on this content are distributed under the same license.

IntechOpen

IntechOpen